DR-2217-9

I-14007

UCID--20033

DE84 009347

GLODEP2: A Computer Model for Estimating Gamma Dose due to Worldwide Fallout of Radioactive Debris

Leslie L. Edwards
Ted F. Harvey
Kendall R. Peterson

March 1984

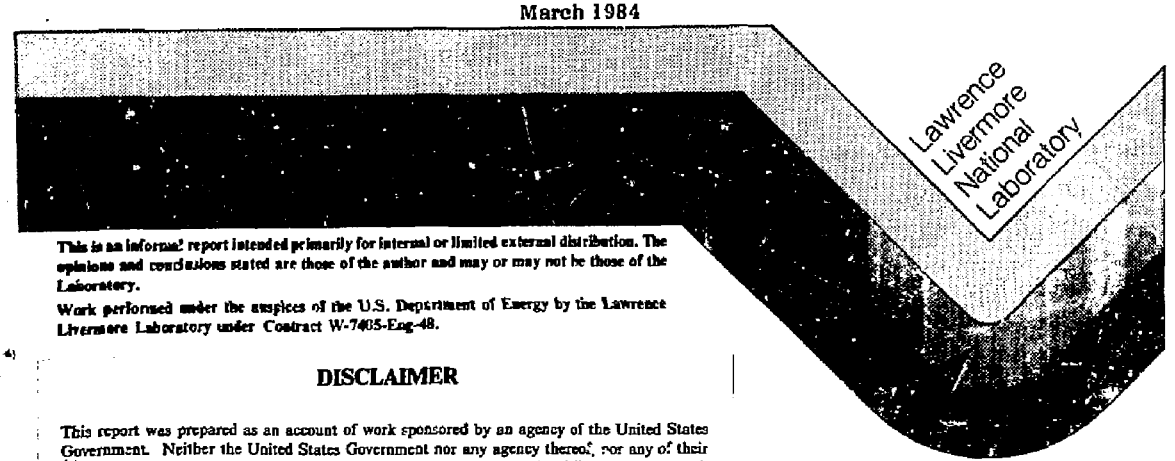

UCID-20033

GLODEP2: A Computer Model For Estimating Gamma Dose due to Worldwide Fallout of Radioactive Debris

Leslie L. Edwards
Ted F. Harvey
Kendall R. Peterson

March 1984

ABSTRACT

The GLODEP2 computer code provides estimates of the surface deposition of "worldwide" radioactivity and the gamma-ray dose to man from intermediate and long-term fallout. The code is based on empirical models derived primarily from injection-deposition experience gained from the U.S. and U.S.S.R. nuclear tests in 1958.

Under the assumption that a nuclear power facility is destroyed and that its debris behaves in the same manner as the radioactive cloud produced by the nuclear weapon that attacked the facility, predictions are made for the gamma dose from this source of radioactivity.

Empirical gamma dose models that account for meteorology, weathering and terrain roughness shielding at specific locations are included.

As a comparison study the gamma dose due to the atmospheric nuclear tests from the period of 1951-1962 has been computed. The computed and measured values from Grove, U.K. and Chiba, Japan agree to within a few percent.

The global deposition of radioactivity and resultant gamma dose from a hypothetical strategic nuclear exchange between the U.S. and the U.S.S.R. is reported. Of the assumed 5300 Mton in the exchange, 2031 Mton of radioactive debris is injected in the atmosphere. The highest estimated average whole body total integrated dose over 50 years (assuming no reduction by sheltering or weathering) is 23 rem in the 30-50 degree latitude band. If the attack included a 100 GW(e) nuclear power industry as targets in the U.S., thus dose is increased to 84.6 rem. "Hotspots" due to rainfall could increase these values by factors of 10-50.

The local unsheltered dose including rainfall, weathering and terrain roughness for grassy fields near non-combatant cities has been estimated for the scenario including the nuclear industry. Results indicate that London, U.K. would receive about 18 rem, Montreal, Canada and Lisbon, Portugal about 22 rem, Tokyo, Japan about 27 rem, and Sydney, Australia about 0.6 rem.

If a large nuclear exchange were to occur and if, in fact, the exchange caused a "nuclear winter" it is probable that the current empirical general circulation and meteorological models would no longer be valid. All of the above results could be changed significantly if such effects greatly changed the fallout and deposition patterns.

1. INTRODUCTION

All nuclear detonations at or above the surface produce atmospheric radioactive debris. Most of this debris is subsequently deposited on the earth's surface from minutes to years after the event. The potential hazard of radioactive fallout was recognized by scientists even before the Trinity test at Almagordo, New Mexico on July 16, 1945 [1]. As is well known, the peacetime testing of nuclear weapons in the atmosphere is capable of producing global contamination and was the subject of intense worldwide concern between 1954 and 1963 when the limited test ban treaty was signed.

Over the past several decades there has been continuing research and debate on the effects of nuclear war. Recently an entire issue of AMBIO [2] was devoted to the topic of the aftermath of nuclear war.

In August 1975 the National Academy of Sciences (NAS) published a study of long-term effects of multiple nuclear weapons detonations [3]. In that report it was noted that

> "In the event of a nuclear exchange, nuclear power related installations such as nuclear power plants, nuclear fuel manufacturing and reprocessing plants, and nuclear waste storage facilities may pose special problems because of the radioactive materials that they contain."

The NAS report does not examine these problems. However, C. V. Chester and R. O. Chester [4] published a study of local fallout from nuclear power facilities in 1976. The AMBIO [2] publication also addresses this problem.

The objective of this report is to document the development of a computer code, GLODEP2, capable of estimating the potential hazard due to gamma-ray dose from radioactive worldwide fallout.

Local fallout occurs mostly downwind of the detonation site on a time scale of hours to a day after the burst and will not be considered in this report.

Intermediate fallout occurs on a time scale of days to a month or two. The debris cloud encircles the globe, perhaps several times, as a diffusing cloud of decreasing radioactivity. This portion of the fallout is contained within the troposphere, the first 9-17 km of the atmosphere. A Gaussian diffusion deposition model is employed to model this fallout.

Long-term fallout is defined as debris initially placed into the stratosphere, or higher, that deposits over the globe on a time scale of months to years after nuclear events. In GLODEP2 this fallout is modeled in essentially the same manner as that reported by Peterson [5] in 1970.

Given the yield, fission fraction, height of burst, latitude and season of each nuclear burst and the type of nuclear installation (if any) involved, the fractional injections into the atmosphere and surface deposition of radioactive debris is predicted. This debris is then converted to a gamma-ray dose to man.

Specific location dose calculations include weathering, penetration and runoff as well as rainfall factors. The models are based on the empirical works of Gale, Humphreys and Fisher [6] and Lowder, Beck and Condon [7].

The decay laws and "dose-area-integral" values for conversion to gamma-ray dose for nuclear power installations are taken from the work of Chester and Chester [4]. The empirical data for the deposition model used in the code are taken from Peterson [5] and are included in Appendix A.

The model descriptions will be delineated in Section 2, the GLODEP2 code description is given in Section 3, sample calculations appear in Section 4, and finally discussion and conclusions are presented in Section 5. A code "Users Guide" is included in Appendix B.

2. EMPIRICAL AND MATHEMATICAL MODELS

This section presents the models used in the GLODEP2 computer code. It is important to note that these models are based on measurements and that all "parameters" are empirical. The computer code as such was not developed using adjustable parameters to be "tuned" to the data.

2.1 Injection Model

Due to lack of knowledge of the detailed relationship between injections into various portions of the atmosphere and subsequent deposition, it is assumed that the atmosphere can be partitioned into compartments such that debris injected into a particular compartment will behave the same irrespective of where in the compartment it is injected. The partitioning is shown in Figure 1. Two latitude bands have been selected: 0-30 degrees North, called equatorial; and 30-90 degrees North, called polar.

Using the same methodology as Peterson [5], the lower boundary of the stratospheric compartments is the tropopause, assumed as 17 km for equatorial regions and 9 km for polar regions. The top compartments extend upward to 300-500 km but a practical limit of 400 km is used in GLODEP2. Results from a 1962 high altitude burst (List et al. [8]) indicate that most of the debris placed initially at or below these levels will not escape the earth's atmosphere and will eventually be deposited on the surface.

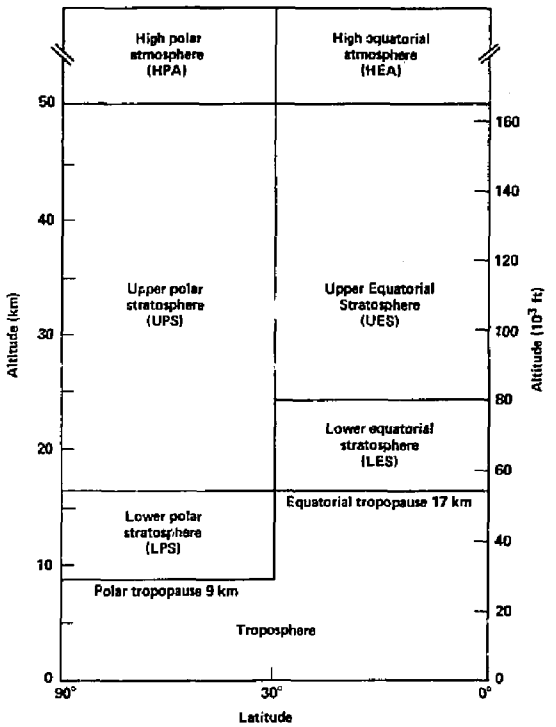

Figure 1. Atmospheric compartments for partitioning nuclear debris. The highest compartments extend to heights so that most of the injected debris will be eventually deposited on the surface (Peterson, 1970).

The tops and bases of the mushroom cap debris clouds are assumed to vary with total yield according to the curves in Figure 2. Peterson based this diagram on equatorial cloud measurements by Ferber [9] and the U.S. Weather Bureau [10]. The polar top and base curves in this figure were estimated by comparisons of equatorial and polar atmospheric stabilities [5]. Additional work by Seitz et al. [11] in 1968 indicate lower cloud values for yields above 3 Mton. In 1979 Telegadas [12] reported studies of the Chinese (PRC) atmospheric tests at 40 degrees North. His curves are based on aircraft samples taken "weeks or months" after each nuclear test, all in the 0.02-4 Mton range. Telegadas' cloud tops above 3 Mton appear to be similar to Peterson's polar tops. See, for example, Figure 3 taken from the 1979 work of Bauer [13].

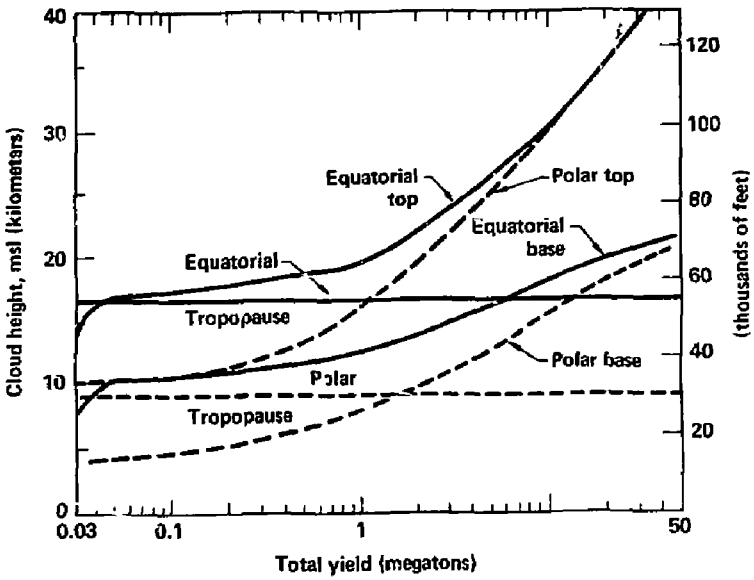

Figure 2. "Mushroom cap" cloud top and base as a function of total yield of device. "Equatorial" refers to 0-30 degrees latitude; "polar" refers to 30-90 degrees (*Peterson, 1970*).

Although there are differences in the values of cloud top and bottom as seen in Figures 2 and 3, we use the Peterson (1970) values in GLODEP2 since he obtained reasonable agreement with deposition measurements. Further, in the sample calculation reported in Section 4.1, excellent agreement with measurements at two locations is shown. This might be an area for further research using GLODEP2. For example, a sensitivity study could be made on the effects of cloud top and bottom values on the dose when one has multiple bursts such as the 19[illegible]62 test series.

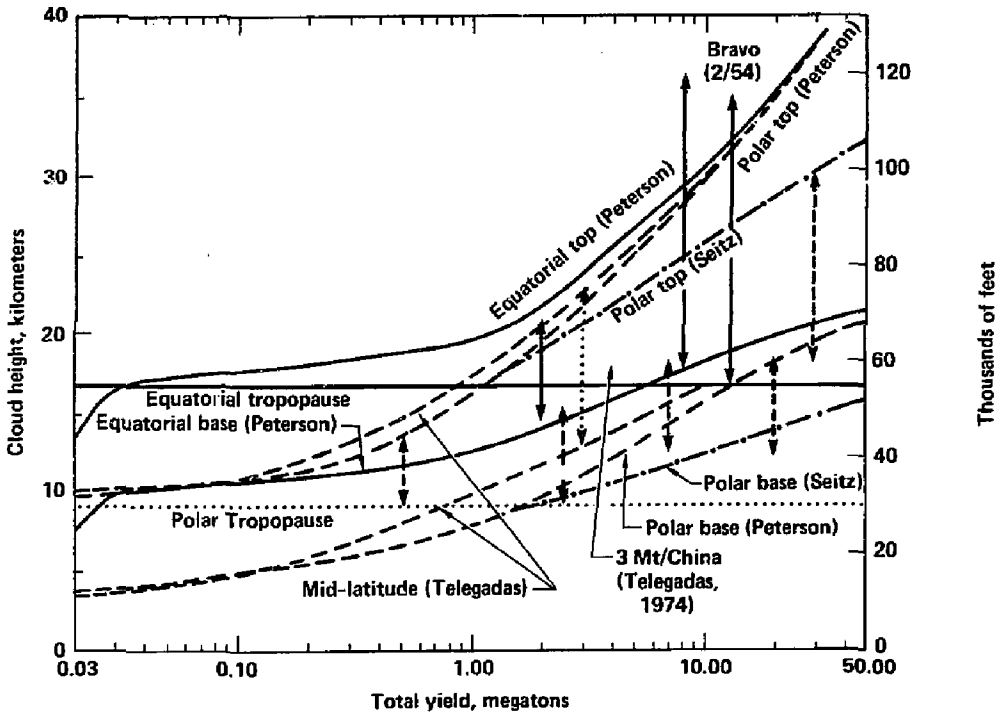

Figure 3. Cloud rise height as a function of yield for different latitudes. United States tests were conducted at equatorial latitude (2°-17°N), Chinese at mid-latitude (40°N), and Soviet at polar latitude (75°N). Peterson's (1970) curves are based on United States tests; all United States explosives had yields below 15 Mtons. Thus Peterson's equatorial curves for yields above 15 Mtons as well as his polar curves are estimates. Estimates of Seitz et al. (1968) for individual United States (solid) and Soviet (dashed) explosions are shown as vertical lines. Dot-dash curves have been drawn by eye through Seitz' Soviet lines to provide an alternative to Peterson's polar case. Note the significant difference for yields greater than 1.5 Mton. Some mid-latitude estimates of Telegadas (1979) are also shown, based on Chinese explosions. (Bauer, 1979.)

The initial vertical distribution of radioactivity within the cloud is a modification of Ferber's [9] distribution into seven equal layers as shown in Table 1. This distribution is used directly for airbursts—those in which the fireball does not touch the surface of the earth—with height-of-burst at 3 km or less. In the remaining cases modifications are made. Based on Table 1, Peterson [5] derived injection tables for both equatorial and polar bursts which are reproduced in *Appendix A, Tables A-1a and A-1b.* These tables are used in GLODEP2 as follows:

The table values are Mtons of total yield injected. These values must be multiplied by the fission fraction, f, of the device to produce actual Mtons of fission products injected.

The fireball radius, R (in meters), of a nuclear burst may be estimated by

$$R = 870\ Y^{0.4}$$

where Y is the device yield in Mton. Let H be the device height-of-burst in meters. Then, if

$R < H \leq 3000$ — use linear interpolation of yield in either Table A-1a or Table A-1b

$0 \leq H < R$ — use a "spherical cap" reduction factor on the table values defined by

$$FR = 1 - (R-H)^2\,(2R-H)/(4R^3) \qquad \text{(Eq. 1)}$$

$3000 < H$ — find cloud top and bottom in the table value for the appropriate yield. Use logarithmic linear interpolation on yield if necessary. Determine an injection per unit height for each of the atmospheric compartments based on the table values. Adjust the cloud upward by the amount (H-3000) meters and apply conservation of amount injected to compute new values of injection in the atmospheric compartments.

Layer, fraction of "mushroom cap" (from base to top)	percentage of activity within layer
0-1/7	1
1/7-2/7	14
2/7-3/7	25
3/7-4/7	25
4/7-5/7	15
5/7-6/7	15
6/7-7/7	5

Table 1. Initial vertical distribution of radioactivity assumed within "mushroom cap."

Thus, for any single nuclear explosion, given

i = quarter of injection
Y = total yield in Mtons
H = height-of-burst in meters
f = fission fraction of the device
d = detonation latitude

then, using the procedure outlined above, compute

R = radius of fireball in meters,
FR = a factor between .5 and 1. for injection reduction if needed (see Eq. 1),

and, using the tables, an injection of fission products, IFP,

$$IFP^{i}_{j,k} = f*FR*Y*(\text{Table value based on d, Y,H})_{j,k} \text{ (Mtons)} \qquad \text{(Eq. 2)}$$

for injection quarter i, atmospheric compartment j,k for

k = either Polar or Equatorial
j = appropriate tropospheric, lower stratospheric, upper stratospheric or high atmospheric compartment.

In the case that a nuclear power installation is attacked, we assume that the entire facility is cratered by a surface burst. We further assume that 50% of the debris is injected into the atmosphere in exactly the same manner as the debris from the nuclear weapon used in the attack.

Thus, if m nuclear power installations of type n are also attacked by the above device, then we also have those fission products injected as the fractional amount of type n facility

$$NFP^{i,n}_{j,k} = 0.5\ m_n * (\text{Table value based on d, Y, H})_{j,k}/Y \qquad \text{(Eq. 3)}$$

with the assumed 50% of the facilities fission products injected due to a ground-burst weapon. The i, j, and k indices have the same meaning as for IFP.

2.2 Deposition Model

In GLODEP2 use is made of Peterson's [5] division of the globe into nine latitude bands of 20 degrees each. Within each band the surface deposition is assumed to be uniform around the entire earth. We are concerned with both the intermediate (tropospheric) and long-term (stratospheric) fallout. The immediate local fallout is not included in the GLODEP2 model.

2.2.1 Intermediate Deposition

It is assumed that the intermediate fallout originates in the tropospheric compartment, and deposition occurs on a time scale of days to a month or two. In the model this portion of the fallout is contained within the first 9 km for a polar injection and the first 17 km for an equatorial injection. We assume the debris cloud encircles the globe, perhaps several times, as a diffusing cloud of decreasing radioactivity. A Gaussian diffusion methodology is employed to model this deposition.

The tropospheric deposition model is based on a Gaussian cloud centered at the detonation latitude with a 10 degree standard deviation. The Gaussian is superposed over the 20 degree latitude bands. A fractional deposition is assigned to the latitude band that agrees with the area under the Gaussian within the band. Reflection techniques at the North Pole are used to conserve the fractional depositions. Fig. 4 illustrates the procedure.

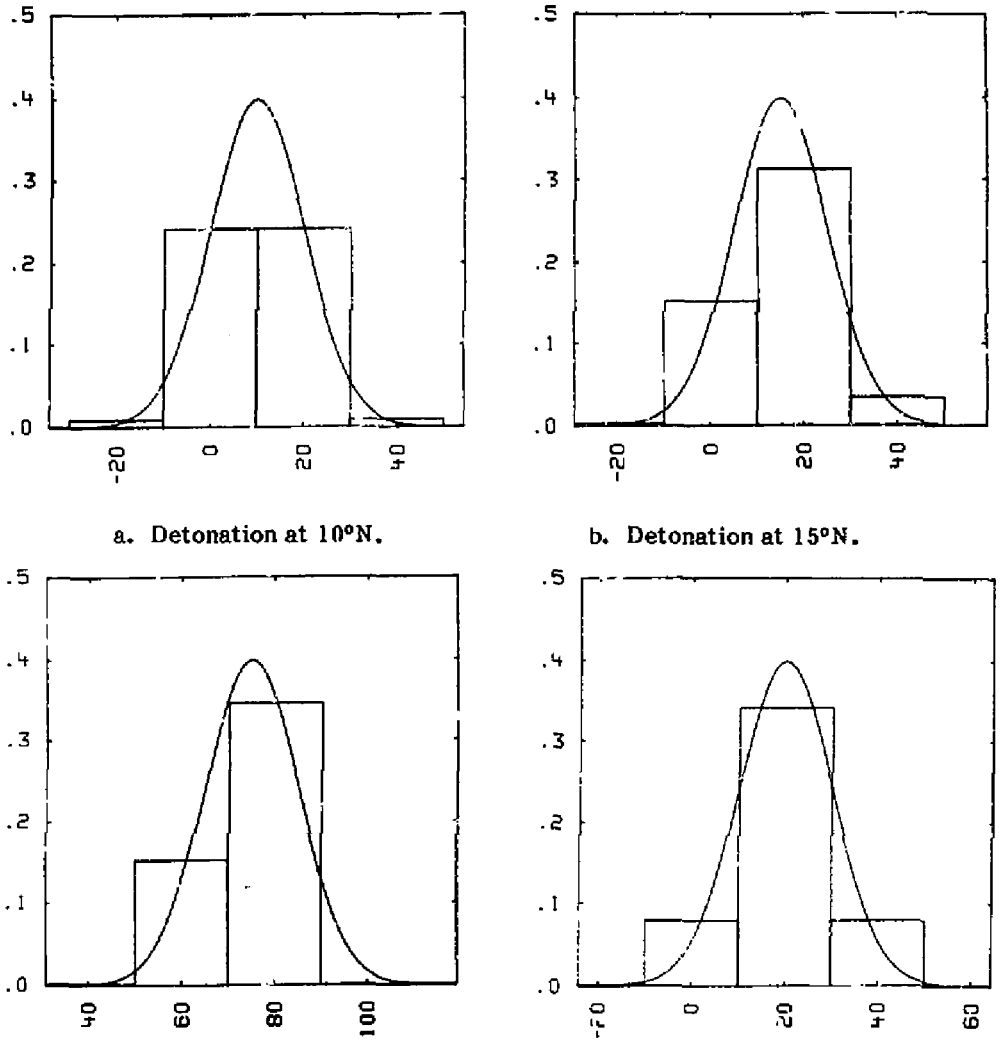

a. Detonation at 10°N.

b. Detonation at 15°N.

c. Detonation at 20°N.

d. Detonation at 75°N.

Figure 4. Tropospheric deposition fractions for 20 degree latitude bands using a Gaussian distribution about the detonation latitude. Reflection techniques are applied at the North Pole as shown in Figure 4d.

The deposition fractions associated with Figure 4 are listed in Table 2. Note that with a Northern Hemisphere injection, and a 10 degree standard deviation on the Gaussian, there is no tropospheric deposition in the two southern-most latitude bands.

Detonation Latitude (Degrees N)	Latitude Band						
	70-90N	50-70N	30-50N	10-30N	10N-10S	10-30S	30-50S
10 (Fig. 4a)	0.	0.	0.0179	0.4821	0.4821	0.0179	0.
15 (Fig. 4b)	0.	0.	0.0668	0.6247	0.3038	0.0047	0.
20 (Fig. 4c)	0.	0.001	0.1577	0.6826	0.1577	0.001	0.
75 (Fig. 4d)	0.6915	0.3038	0.0047	0.	0.	0.	0.

Table 2. Examples of fractional deposition of tropospheric fallout.

Figure 5, taken from the work of Machta, as reported in [14], indicates that measurements of tropospheric fallout are very close to Gaussian with about a 10 degree standard deviation.

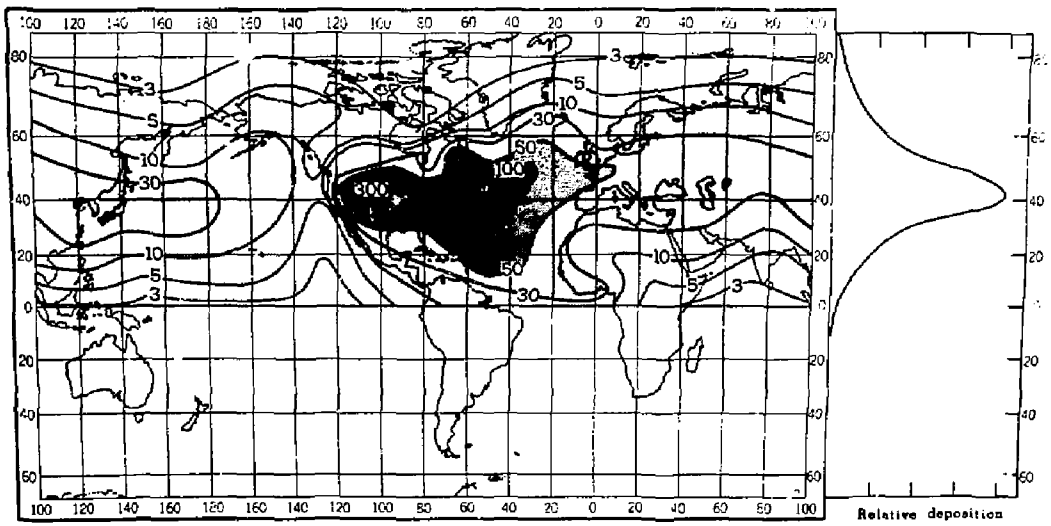

Figure 5. Worldwide fallout of radioactivity from nuclear weapons tests in Nevada in 1953. The explosions were in the kiloton range of yields, and debris was confined to the troposphere. The intensity of fallout is shown in relative units (L. Machta).

Since the intermediate fallout always occurs during the first quarter after injection, GLODEP2 allows input of a fraction of the quarter at which time deposition is complete. Then, given the injection of fission products and computing the latitude fractional depositions as above, the surface deposition, WSD, from the troposphere is computed as

$$WSD^{i}_{j,k,b} = IFP^{i}_{j,k} * FD_{b} \text{ (Mtons of weapons debris deposited)}$$

where

$IFP^{i}_{j,k}$ is the Mtons of weapons fission products injected (see Eq. 2),

FD_{b} is the fractional deposition,

and

i is the injection quarter,

k=1 for equatorial, =2 for polar,

j=1 for tropospheric compartment,

b=1,2,....9 for the 20 degree latitude bands from North to South.

In case of attack on a nuclear power installation, the relative amount of the fission products deposited, NSD, is computed by

$$NSD^{i,n}_{j,k,b} = NFP^{i,n}_{j,k} * FD_{b} \text{ (relative amount of type n deposited)}$$

where n is the index for the type of nuclear facility and

$NFP^{i,n}_{j,k}$ is the fractional facility injected in compartment j,k (see Eq. 3).

The remaining indices are as above.

2.2.2 Long-Term Fallout and Deposition

The GLODEP2 fallout model for long-term deposition is identical with that derived by Peterson [5] based on injections of tracer elements as shown in Table 3.

Compartment	Data source and injection date	First deposition	Maximum deposition	First half of deposition	Partitioning between hemispheres
Lower equatorial stratosphere	^{185}W (May-Aug 1958)	1st season	1st spring	8 months	2:1
Upper equatorial stratosphere	None	(1st spring)	(2nd spring)	(2 yr)	(1:1)
High equatorial atmosphere	^{102}Rh (Aug 1958) ^{109}Cd (July 1962) ^{238}Pu (April 1964)	2nd spring	3rd spring	3-1/2 yr	2-1/2:1
Lower polar stratosphere	$^{89}Sr/^{90}Sr$ ratios (Oct. 1958)	1st season	1st spring	5 months	20:1
Upper polar stratosphere	^{54}Mn (1961-62)	Within 6 months	2nd spring	2 yr	4:1
High polar atmosphere	None	(2nd spring)	(3rd spring)	(3-1/2 yr)	(2:1)

Table 3. Source of tracer data with date of injection and parameters used to prepare deposition tables; parentheses indicate subjective estimates for compartments lacking tracer data (Peterson, 1970).

Table 3 indicates information germane to deposition from the various compartments. The parentheses show where "subjective estimates" were necessary since observations were not available. The third column shows the time required for stratospheric debris to first reach the surface. As would be expected, this time increases with height of injection.

The fourth column shows the time after injection for the occurrence of the maximum seasonal deposition. Although the Lower Polar compartment yields relatively higher maximum deposition values than the adjacent equatorial compartment, the time of the maximum is the same and increases with altitude.

The estimated partitioning between the Northern and Southern Hemisphere within each compartment is shown in the last column.

From the information shown in Table 3, Peterson constructed deposition tables for those compartments within which unique tracer information was not available. Thus, fractional deposition tables were prepared for all injection quarters for all of the stratospheric and high atmospheric compartments. These tables are reproduced in Appendix A.

Then, given the fission products injected in quarter i, at detonation latitude, d, the surface deposition from the stratospheric and high atmospheric compartments in latitude band b are computed by

$$WSD_{j,k,b}^{i+q} = IFP_{j,k}^{i} * \ FD_{j,k,b}^{i,q} \text{ (Mtons of weapons debris deposited)}$$

where FD is the fractional deposition from the appropriate table (tables A-2a thru A-7b), and

q = 0,1,2....23 is the quarter after injection,

j = 2 for deposition from the lower stratospheric compartment,

= 3 for deposition from the upper stratospheric compartment,

= 4 for deposition from the high atmospheric compartment,

k = 1 for equatorial injection, =2 for polar injection,

and b = 1,2....9 for the latitude bands from North to South.

In case of attack on a nuclear power installation, we also compute

$$NSD_{j,k,b}^{i+q,n} = NFP_{j,k}^{i,n} * \ FD_{j,k,b}^{i,q} \text{ (Relative amount of type n deposited)}$$

where NFP is the fraction of type n facility injected and the indices are the same as above.

Note the similarity to the equations used for the tropospheric deposition in the preceding section. The only difference is that the superscript q=0 for the tropospheric (intermediate) deposition, all of which occurs in the first quarter.

2.3 Gamma-Ray Dose Models

2.3.1 "Uniform" Dose Over Latitude Bands

The curves in Figure 6 from [4] show the gamma-ray dose rate versus time after detonation for a 1-Mton fission weapon (1-MT), the equilibrium core of a light water reactor (CORE), the inventory associated with a 5-ton per day nuclear fuel reprocessing plant that has 10 years of stored high-level waste (HLW), and 10-years of spent fuel stored at a LWR (SF). The units have been converted to (rem - km^2)/qtr.

For any given deposition quarter, p, numerical integration under the n-th curve, yields

d_n^p in (rem-km^2)/(unit of device type n) per quarter

as a "dose-area-integral" that properly accounts for the decay law associated with the weapon or nuclear installation.

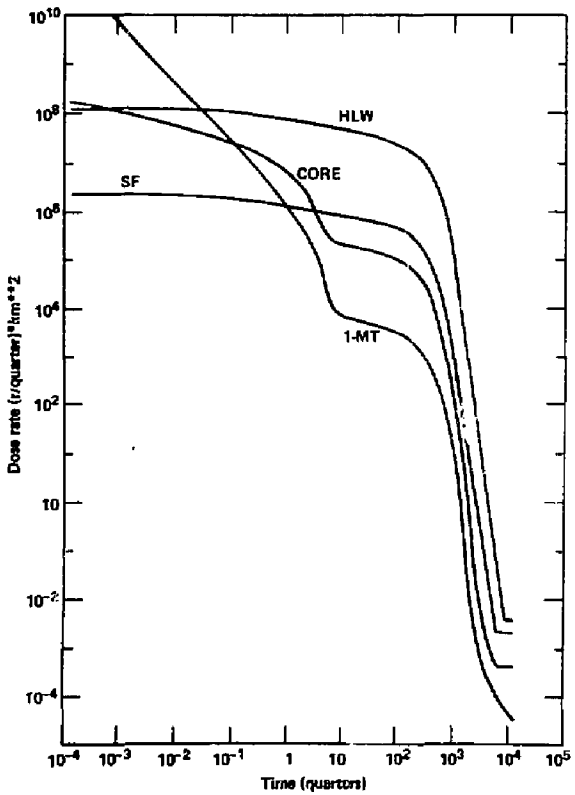

Figure 6. Gamma-ray dose area integral rate versus time after shutdown or detonation (Chester and Chester, 1976).

We assume a delta function deposition of debris

$$WSD_{j,k,b}^{i+q} \text{ (weapon) or } NSD_{j,k,b}^{i+q,n} \text{ (type n facility)}$$

at the mid-quarter, i+q. Then for a single burst injection, the quarterly dose rate in the p-th quarter due to the deposition in the current and earlier quarters is given by

$$\dot{D}_b^{p,n} = d_n^p \sum_{i+q=1}^{i+q<p} \sum_{k=1}^{k=2} \sum_{j=1}^{j=4} (WSD \text{ or } NDS)_{j,k,b}^{i+q,n} / A_b \text{ (rem/qtr)}$$

where A_b is the area (km^2) of the b-th latitude band.

If there are multiple bursts or several nuclear power installations then summation over all of them produces a "total quarterly" dose rate in the p-th quarter and b-th 20 degree latitude band.

Define lower and upper limits for dose exposure by

pi = beginning quarter to start dose exposure, and

pf = final quarter for dose exposure,

e.g., 0 and 200 for a 50-year dose, or, 9 and 10 quarters for a 6 month dose starting 2 years after detonation, then the accumulated gamma-ray dose is computed by

$$D\,(pi,pf)_b^n = \sum_{p=pi}^{p=pf} \dot{D}_b^{p,n} \text{ (rem)}$$

for the n-th fission product source and the b-th latitude band. A sum over all the n injection sources produces a final gamma dose from pi through pf.

2.3.2 "Location" Dose with Weather, Terrain, Penetration and Run-off

Predicting a dose at a specific location requires consideration of all the significant local factors. Factors we have identified are terrain roughness shielding, average local rain rate, runoff and soil penetration. To compare with observed gamma radiation fields due to atmospheric testing requires inclusion of these factors in the model used for the predictions.

To incorporate the effects of non-smooth terrain, the recommendation of Glasstone and Dolan [15] is used. They propose a dose-area integral reduction of thirty percent due to terrain roughness and vegetation shielding. That is, we define a terrain roughness factor, F_T, where, for moderately rough terrain,

$$F_T = 0.7$$

which reduces the uniform dose rate of the preceding section.

The effect of rainout on accumulation of radioactivity at different locations is widely observed. The greater the rainfall at a site, the larger the deposition of tropospheric radioactivity. In fact, for long-range fallout, nearly all of the radioactivity is deposited by rain systems. The GLODEP2 model takes this into account by providing a longitudinal variation to the latitudinal model predictions based on the rain rate at a given longitude. To establish the relation between average annual rain rate and deposition rate we use data accumulated by Lowder et al. [7] as shown in Figure 7. The implication of these data is that the deposition of radioactivity is proportional to the annual average rain rate to the three-fifths power. Thus, to first order, the ratio of the local rate of deposition to the uniform rate for a latitude band is equal to the ratio of the local rain rate to the rain rate averaged over the latitude band to the three-fifths power. Hence, we define another factor, F_R (R, R'), where

$$F_R (R,R') = (R/R')^{0.6}$$

where R is the rain rate at a specific location and R' is the latitude band average rain rate.

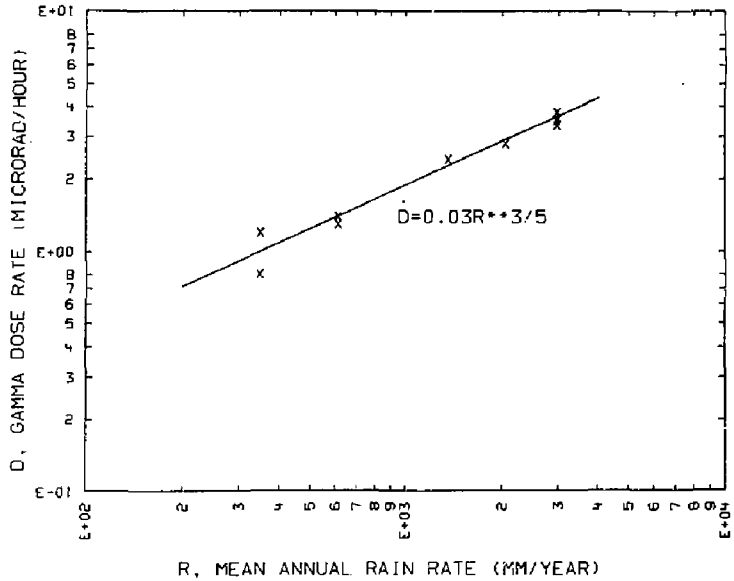

Figure 7. Gamma dose rate (microrad/hr) vs. mean annual rain rate (mm/y) as measured by Lowder, et al. [7].

After deposition, radioactive nuclear debris migrates, albeit at times very slowly. Thus, to make predictions which compare reasonably with observations, account must be taken of the migration. In this model we empirically account for penetration and runoff for the simple case of a grassy field. The best data is available for this case. Scenarios such as runoff for metropolitan areas are extremely complex and beyond the scope of this work. Consequently, our dose predictions should not be considered appropriate for metropolitan areas, but for typical grassy fields. The person receiving the dose is assumed not to be shielded and remains in the location for the entire period of dose exposure.

Measurements of weathering of ^{137}Cs has been made in England by Gale et al. [6]. We have modified Gale's expression to take into account the different precipitation rates at other locations. The ^{137}Cs tends to be tightly bound to the soil particles on which it is deposited. Gale et al. have split the ^{137}Cs into 63% which migrates fairly easily and 37% which tends to be fairly closely bound to its deposition site. We assume the same split for all the radionuclides. We realize that this assumption may be in error if one considers the fact that the "nuclide retardation factors" vary over several orders of magnitude, dependent on the chemical properties of the nuclide, the nature of the soil, the nature of the water in the soil, etc. To model these features in detail introduces a complexity that is beyond the capabilities of the current GLODEP2 model.

We include the rain rate as a linear proportionality in the weathering reduction, by defining the weathered dose factor, $F_W(t,R)$, as

$$F_W(t,R) = 0.63\exp(-0.693Rt/41.8) + 0.37\exp(-0.693Rt/6320)$$

where t is the time after deposition and R is the local average annual rain rate.

Finally, the dose rate at a specific location is computed by assuming the uniform dose rates of the preceding section are located at the center of the latitude band. A linear interpolation to the local latitude produces an "unweathered, smooth terrain" rate, $D'(t)$. The final expression for unsheltered, weathered, grassy terrain dose rate at a specific location is

$$D_W(t,R,R') = F_T^* \; F_R^* \; F_W^* \; D'(t)$$

at time t after deposition

3. GLODEP2 CODE STRUCTURE AND COMPUTATIONAL ALGORITHMS

The current version of GLODEP2 is written for the CRAY-1 computer using the LRLTRAN language. The number of subscripts used, certain of the input statements and the graphics package are not directly adaptable to FORTRAN IV language. Input to the code may be accomplished using an input disk file (see APPENDIX B) or by teletype in a conversational mode.

In this section the basic code structure and the computational algorithms are delineated.

3.1. Modular Code Structure

As depicted in Figure 8, GLODEP2 is structured in a modular form to allow further development of models as required with minimum disturbance to the remainder of the code.

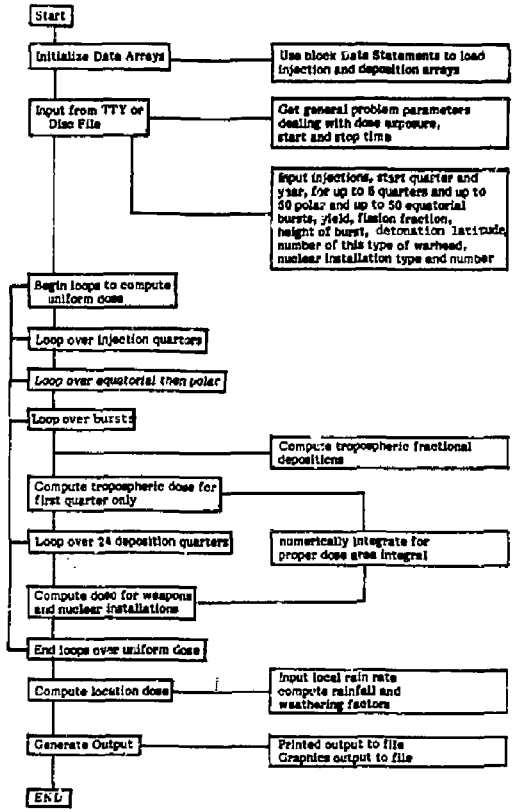

Figure 8. Modular structure of the GLODEP2 computer program.

3.2 Data Arrays

Peterson's [5] deposition arrays are converted from ^{90}Sr values given in [5] to pure fractions. The standard FORTRAN IV BLOCK DATA statements are used to load:

FINJ(i,j,k), injection tables A-1a and A-1b, where

i=1, 17 is a function of total yield in Mtons
j=1 is device total yield
=2 is debris cloud top (km)
=3 is debris cloud bottom (km)

and for

		k=1 (equatorial)	k=2 (polar)
j=4	is Mton of total yield injected	0-17 km	0-9 km
=5	is Mton of total yield injected	17-24 km	9-17 km
=6	is Mton of total yield injected	24-50 km	17-50 km
=7	is Mton of total yield injected	>50 km	>50 km

DTABS(i,j,k,m), surface deposition tables A-2,3,5 and 6, where

i=1,24 for the 24 quarters of deposition
j=1,9 for the 9-20 degree latitude bands from North to South
k=1 for injections during Dec-Feb
=2 for injections during Mar-May
=3 for injections during Jun-Aug
=4 for injections during Sep-Nov
m=1 is fractional deposition from LES (tables A-2a,b,c and d)
=2 is fractional deposition from UES (tables A-3a,b,c and d)
=3 is fractional deposition from LPS (tables A-5a,b,c and d)
=4 is fractional deposition from UPS (tables A-6a,b,c and d)

DTABA(i,j,k,m), surface deposition tables A-4 and 7, where

i and j are as above, and
k = 1 for injections during Mar-Aug
= 2 for injections during Sep-Feb
m = 1 is fractional deposition from HEA (tables A-4a and b)
= 2 is fractional deposition from HPA (tables A-7a and b).

These tables are basically fractional depositions for the amount of radioactive debris remaining in the appropriate compartment. If the fractional values in any given table (and their indicated extensions) are summed, the sum is very near unity.

3.3 Injection Algorithms

The assumed input consists of

Y = total yield of the device (Mtons)

H = height-of-burst of the device (meters)

NW = number of warheads of this type of device at this location

f = fission fraction of the device

d = detonation latitude of this device

n =0 if no attack on a nuclear power installations with this device

=1 if attack on reprocessing plant

=2 if attack on *30-day spent fuel storage facility*

=3 if attack on 3600 MW(th) LWR, (steady state)

=4 if attack on 10-yr spent fuel storage at reactor facility

NF = *number of nuclear facilities of type n.*

Then compute

I = 1 if $0 \leq d \leq 30$, an equatorial injection

= 2 if $30 < d \leq 90$, a polar injection,

R = $870\ Y^{0.4}$

0.5 if H=0

FR = { 1.0 if $H \geq R$

$1.-(H-R)^2\,(2R-H)/(4R^3)$ if $0 < H < R$,

a height-of-burst factor.

Next the fractional injections are computed using the appropriate table FINJ(i,j,I). If I=1, then IB=16, otherwise, IB=17, and

if Y < FINJ(1,1,I), set IN=1 and X=0,

if Y > FINJ(IB,1,I), set IN=IB and X=0,

if Y = FINJ(i,1,I), set IN=i and X=0, otherwise

if FINJ(i,1,I) < Y < FINJ(i+1,1,I), set IN=i and X=(Y-FINJ(i,1,I)/

(FINJ(i+1,1,I)-FINJ(i,1,I).

Then, using the interpolation if necessary, obtain the injection fractions by

x(i)=FINJ(IN,i,I) + X* (FINJ(IN+1,i,I)-FINJ(IN,i,I))

for i=1, troposphere
=2, lower stratosphere
=3, upper stratosphere
=4, high atmosphere.

If H > 3000, adjust the x(i) by the amount DH=H-3000 as follows:

Let XL = 0 if X=0, otherwise
XL = (log(Y/FINJ(IN,1,I))/log(FINJ(IN+1,1,I)/FINJ(IN,1,I)),

and compute cloud top and bottom

ct=FINJ(IN,2,I)+XL (FINJ(IN+1,2,I)-FINJ(IN,2,I))
cb=FINJ(IN,3,I)+XL (FINJ(IN+1,3,I)-FINJ(IN,3,I)).

The new cloud top and bottom are then defined to be

ctn=ct+DH
cbn=cb+DH

Next adjust the x(i) values by conservation of injection. For example if I=1 and cb < 17, ct > 17, cbn < 17, then

x(1)=x(1) (17-cbn)/(17-cb) and
x(2)=x(2)+x(1) (cbn-cb)/(17-cb).

The remaining levels would also be adjusted by the same technique.

Then, for each burst of injection information, store the array

RINJ(q,L,i,j), where

q=quarter of injection, $1 \leq q \leq 6$, and q=1 corresponds to the start of injection quarter and year,

I=1 is equatorial, =2 is polar,

i=burst number for this quarter, $1 \leq i \leq 50$,

j=1 is x(1), fractional injection into the troposphere,

=2 is x(2), fractional injection into the lower stratosphere,

=3 is x(3), fractional injection into the upper stratosphere,

=4 is x(4), fractional injection into the high atmosphere,

=5 is Y* NW, total yield in Mtons for this burst,

=6 is n, the type of nuclear installation,

=7 is f* FR, the fission product reduction factor,

=8 is NF, the number of type n installations, if any,

=9 is d, the detonation latitude.

3.4 DEPOSITION ALGORITHMS

3.4.1 Intermediate Fallout

The intermediate deposition from the troposphere occurs on a time scale of days to a month or two. We assume the deposition occurs at an "input" fraction of the first quarter and that it can be modelled using a Gaussian distribution about the detonation latitude, d. The fractional deposition i. to the 20 degree latitude bands assuming a 10 degree standard deviation on the Gaussian is computed.

A function, GETA(x), is defined to use linear interpolation on a standard normal (0,1) set of data to get the area under the Gaussian curve from 0 to the distance x.

The computation is then done as follows:

For any given burst, i, in quarter q, we have from above,

d=RINJ(q,I,i,9), the detonation latitude, and

fi=RINJ(q,I,i,1), the fractional injection in the troposphere.

We then determine the latitude band in which d is located, i.e., b' such that

$(90-20\,(b'-1)) \geq d > (90-20\,b')$,

then

if b' = 1, xhi=3.4 (to reflect at North pole)

if b' = 1, xhi=[90-20 (b'-1)-d]/10

if b' ≠ 5, xlo=[d-(90-20 b')]/10

if b' = 5, xlo=[d+10]/10 (to compute about the equator),

and then

FRD(b')=GETA(xhi)+GETA(xlo) (area above d + area below d in band).

if b' = 1, then set

xhi=[90-d]/10 if $d \leq 56$

xhi=3.4 if $d > 56$ (to reflect at North Pole)

and compute

FRD(1)=GETA(xhi)-GETA([70-d]/10)-GETA([90-20 b-d]/10).

For b=5 and b ≠ b', about the equator, compute

FRD(5)=GETA([10-d]/10)+GETA([10+d]/10).

For b=6 and 7,

FRD(b)=GETA([d+10+20 (b-5)]/10)-GETA([d+10+20 b]/10).

Since with a Northern Hemisphere detonation and a standard deviation of 10 degrees about d, there will be no significant area in the two southern-most bands; set

FRD(8)=FRD(9)=0.

Finally, the surface deposition due to intermediate fallout from the troposphere for this burst at latitude d is calculated by first computing the FRD array as above, then multiplying by the tropospheric injection. That is, a fractional deposition for this burst is computed by

$TFD(q,I,i,b)=FRD(b)*RINJ(q,I,i,1)$.

This calculation is repeated over the injection quarters, q=1,6; the equatorial, I=1, and polar, I=2; and over all i bursts within each q and I.

3.4.2 Long-Term Fallout

The long-term deposition from the lower stratosphere, upper stratosphere and high atmosphere is done directly using the data-loaded tables. An input start quarter, iq, is assumed where

iq=1 if first injection in Dec-Feb
iq=2 if first injection in Mar-May
iq=3 if first injection in Jun-Aug
iq=4 if first injection in Sep-Nov.

The q=1 corresponds to iq, q=2 to iq+1,....,q=6 to iq+5. To select the proper deposition table, set

iq=iq+(q-1) if iq $\leq$ 4
iq=iq+(q-1)-4 otherwise,
kq=1 if iq=2 or 3,
kq=2 if iq=1 or 4.

For each of the q injection quarters and for I=1 and I=2, and for each of the i bursts within each q and I, compute

SFD(q,I,i,b,n,1)=DTABS(n,b,iq,2 *(I-1)) *RINJ(q,I,i,2), the fractional deposition from the lower stratosphere.

SFD(q,I,i,b,n,2)=DTABS(n,b,iq,2* I) *RINJ(q,I,i,3), the fractional deposition from the upper stratosphere,

SFD(q,I,i,b,n,3)=DTABA(n,b,kq,I) *RINJ(q,I,i,4), the fractional deposition from the high atmosphere,

where n=1,2,...,24 for the deposition quarters, and b=1,2,...,9 for the 20 degree latitude bands from North to South.

3.5 GAMMA DOSE MODEL ALGORITHMS

3.5.1 "Uniform" Dose Over Latitude Bands

The curves in Figure 6 in Section 2.3.1 show the gamma-ray dose rate versus time after detonation or shutdown for

N=1, a 1-Mton fission weapon,
N=2, a reprocessing plant, 10-yr high-level waste storage,
N=3, 30-day spent fuel storage
N=4, 3600-MW(th) LWR (steady state)
N=5, 10-yr spent fuel storage at reactor.

In GLODEP2 we assume that these curves may be represented by piecewise functions of time of the form

$q(t)=q(t1)\ (t-t1)^X$ for the space $t1 \leq t \leq tu$.

Taking the logarithm, we obtain the slope in log-log space,

$x=\log[q(tu)/q(t1)]/\log[tu/t1]$.

Then, the area under the curve from some value, tlo, to the higher value thi. is the sum of the piecewise integrations.

Enough points have been "data-loaded" to reasonably approximate the curves of Figure 6. Thus we can generate the arrays

TG(L), an array of times in quarters, L=1,73, and

G(N,L), an array of dose rates in $(rem \cdot km^2)$/quarter

for the N=1,5 as above, and L=1,73. Then, given the N, tlo and thi, compute the "dose-area-integral" as follows:

Determine

L' such that $TG(L') \leq tlo < TG(L'+1)$, and
L'' such that $TG(L''-1) < thi \leq TG(L'')$,

then, for

$L=L'$, set $tl=tlo$,
$L=L''$, set $th=thi$,
$L' < L < L''$, set $tl=TG(L)$ and $th=TG(L+1)$.

For $L=L', L'+1,\ldots,L''$, compute
$XL=\log[G(N,L+1)/G(N,L)]/\log(TG(L+1)/TG(L))$.
if $XL = -1$, then
$DAI(N,tl,thi) = DAI(N,tlo,thi) + G(N,L)(th^{XL+1}-tl^{(XL+1)})/(XL+1)$.
If $XL = -1$, then
$DAI(N,tlo,thi)=DAI(N,tlo,thi)+G(N,L)\log(th/tl)$.

In the computation of dose, assume p', the quarter in which to start dose exposure, and p'', the quarter after which the dose integration ends are given. For example, a 50-year dose starting immediately after injection would have $p'=0$ and $p''=200$. Further assume that the intermediate deposition occurs in the first quarter, p', starting at some fraction of the quarter, pf.

For each burst, i, in injection quarter q, and for both equatorial, I=1, and polar, I=2, and for each latitude band, b, compute dose rates for the p-th quarter, $p=p',\ldots,p''$, as follows:

For the tropospheric deposition, if $p'=1$, then

$$DDOTH(p,q,i,I,b,N,1)=DAI(N,pf,1)*TFD(q,i,I,b)*FM$$

where FM = RINJ(q,I,i,5)*RINJ(q,I,i,7) if N=1, (=Y*NW*f*FR for weapons)
= RINJ(q,I,i,8) if $N \neq 1$, (=NF, the number of nuclear installations of type N, where N=RINJ(q,I,i,6)+1).

If $p' > 1$, then DDOTN(q,i,I,b,N,1)=0.

Similarly, for the long-term deposition, compute for

p=maximum(p',n) through p=p'', and for
n=1 through n=minimum(24,p'')

$$DDOTN(p,q,i,I,b,N,n)=DAI(N,p-1,p)\ *[SFD(q,I,i,b,n,1)+SFD(q,I,i,b,n,2)+SFD(q,I,i,b,n,3)]*FM$$

where FM is as above.

If the DDOTN are summed over all N,q,i and I, then divided by the area of the latitude band b, we obtain a quarterly dose rate

DDOT(p,b) (rem/qtr) for the band b, b=1,2,...,9 and for the p-th quarter, p=p', p'+1,...,p''.

Finally, summing over the quarters, p=p', p'+1,...p''' gives the accumulated "uniform" gamma-ray dose

$$REM(b,p''') = \sum_{p=p'}^{p'''} \sum_{i=1}^{6} \sum_{q=o}^{23} \sum_{I=1}^{2} \sum_{N=1}^{5} \sum_{n=1}^{4} DDOTN(p,q,i,I,b,N,n)/AREA(b)$$

for latitude band b through quarter p'''.

3.5.2 "Location" Dose

The dose at a specific location is computed using both the local average rainfall and an average rainfall in the latitude band. For computational purposes we have data-loaded the array *rainl(2,k)* using Figure 9.6 on page 370 of Lamb [16]. Here rainl(1,k) is the latitude of measurement k, and rainl(2,k) is the average annual rainfall in mm as shown in Table 4.

Latitude Measurement	Average Annual Rainfall (mm)
85 N	115
75 N	210
65 N	430
55 N	740
45 N	915
25 N	540
15 N	1140
5 N	1860
5 S	1430
20 S	1090
25 S	860
35 S	920
45 S	1200
55 S	1030
65 S	430
75 S	100
85 S	30

Table 4. Latitude of measurement and average annual rainfall measured as extracted from Figure 9.6 of [16].

Given the local latitude, dl, and the average local rainfall, r, in mm, then linear interpolation in Table 4 is used to obtain a latitude average rainfall, r', at dl.

To account for run-off and penetration, a modified version of the model proposed by Gale [6] is used. We compute a reduction factor, FRP, by

$$FRP(p,n)=0.63\exp(-(4.14e-4)\ R\ t)+0.37\exp(-(2.74e-6)\ R\ t)$$

where t is the time in quarters since deposition, i.e., p-n for the factor in the p-th dose quarter for the n-th quarters deposition. The modification to the Gale model is only in the coefficients in the exponentials. Here we have divided Gale's coefficients by the average annual rainfall in Grove, U.K., and converted to time in quarters.

To account for the rate of deposition due to local rainfall, define a deposition factor, *FRF*, based on data taken by Lowder, et al., [7]. Thus

FRF=(R/R') 0.6

is a rainfall multiplication factor.

Glasstone [15] suggests that a "terrain roughness" factor, RF, of about 0.7 should be used to reduce theoretical values to that actually observed in measurements for moderately rough terrain.

Assume that the uniform quarterly dose rate DDOTN(p,q,i,l,b,N,n) of the previous section is located at the center of the 20 degree band; then let:

cl(b) = 90 - 20*(b-1).
then, if cl(b') $\leq$ dl < cl(b'+1), let
dl'=dl-cl(b'), and
dl''=cl(b'+1)-dl

be the linear interpolating distances. The local quarterly dose rates are computed by

DDOTNL(p,q,i,l,dl,N,n)=FRP(p,n)*FRF*RF*[dl''*DDOTN(p,q,i,l,b',N,n)
/AREA(b')+dl'*DDOTN(p,q,i,l,b'',N,n)/AREA(b'')]/(dl'+dl'').

As before, summation over q,i,l,N and n, gives the quarterly dose rate for specific location dl, gives

DDOTL(p,dl) (rem/qtr) for the p-th quarter.

Summation over the quarters, p=p', p'+1,...p''' gives the accumulated gamma-ray dose at the specific location, dl, with R mm of local rainfall

$$REM(b,p''') = \sum_{p=p'}^{p'''} \sum_{i=1}^{6} \sum_{q=o}^{23} \sum_{l=1}^{2} \sum_{N=1}^{5} \sum_{n=1}^{4} DDOTNL(p,q,l,b,N,n)$$

through quarter p'''.

4. SAMPLE CALCULATIONS WITH GLODEP2

In this section two calculations performed with the GLODEP2 code are presented. The first is a series of runs based on the atmospheric nuclear tests of devices over 100 ktons during 1951-1962 [17]. This calculation provides a code comparison with data.

The second calculation deals with the gamma-ray dose effects that would be expected in the case of a large scale nuclear exchange between the U.S. and the U.S.S.R. [17,18].

4.1 1951-1962 ATMOSPHERIC TESTS

Using tables such as those in Appendix B of Glasstone [15], Table 2 of Bauer [13] and Table 1 of the 1982 UNSCEAR [19] report, a series of calculations based on the atmospheric tests during the period of 1951-1962 have been constructed. Only those tests with yields greater than 100 kton have been used since lower values will not inject significant amounts of radioactive debris into the stratosphere. The atmospheric tests conducted by the French and Chinese have been omitted since significant deposition due to the tests would occur after the 1967 time period of interest. Table 5 depicts the number of atmospheric nuclear tests in approximate ranges of total yield as used in our study.

	Approximate Total Yield (Mtons)							
Year	.1-.29	.3-.49	.5-.99	1.-1.9	2.-4.9	5.-9.9	10.-19.9	20.-60.
1951	1	0	0	0	0	0	0	6
1952	0	0	1	0	0	0	1	0
1953	0	1	0	0	0	0	0	0
1954	1	0	0	1	0	0	3	0
1955	1	0	0	1	0	0	0	0
1956	1	2	0	2	4	0	0	0
1957	2	0	3	2	2	0	0	0
1958	6	6	3	7	8	4	0	0
1961	1	1	3	4	7	1	1	1
1962	9	3	10	5	9	4	3	4
Total	22	13	20	22	30	10	0	5

Table 5. Number of atmospheric nuclear tests and approximate ranges of total yield in Mtons for the years 1951-1962.

To compare with measurements at Grove, U.K. [20] for 1951-1967, and at Chiba, Japan [21,22,23,24] for 1962-1967, the accumulated uniform dose for these periods is calculated. Gamma dose with weathering, run-off, penetration and roughness are then computed at these locations.

Table 6 is a summary of the uniform gamma dose accumulted through 1967 for each of the nine 20-degree latitude bands numbered from North to South. The table values are in mrem.

	Latitude Band								
Source	1	2	3	4	5	6	7	8	9
U.S.	11.0	46.7	77.4	111.4	93.8	28.	37.4	27.9	2.6
U.K.	1.7	7.	10.4	32.5	88.6	18.3	4.2	3.2	0.02
U.S.S.R.	302.3	242.5	293.4	83.2	8.6	9.1	18.5	12.6	2.
Total	315.8	296.2	381.2	227.1	191.	55.4	60.1	43.7	4.62

Table 6. Uniform gamma-ray dose (mrem) accumulated through 1967 for atmospheric nuclear tests of 1951-1962.

The gamma dose as measured and computed at two specific locations are shown in Table 7. The agreement, even though it may be somewhat fortuitous, is remarkably good.

We acknowledge that our penetration, run-off and rainfall models are derived primarily from measurements at Grove. However, large portions of these data were obtained from independent, controlled experiments. Further, the injection and deposition models are independent of these data.

We do note that the values computed for Chiba use the GLODEP2 models directly with no fitting of parameters to the measurements reported there.

	Grove, U.K.	Chiba, Japan
Latitude	55.0N	35.5N
Local average Rainfall (mm)	683	1560
Latitude Average Rainfall (mm)	843	730
Computed dose (mrem)	140	124
Measured dose (mrem)	131	122

Table 7. Measured and Computed gamma doses at Grove, U.K. (accumulated from 1951 to 1962), and at Chiba City, Japan (accumulated from 1962 to 1967).

4.2 HYPOTHETICAL LARGE-SCALE NUCLEAR WAR

A study of the available strategic inventories of the two superpowers indicates that about 14000 Mton is hypothetically available, but a more likely, but not implausible, strategic exchange is about 5300 Mton. This exchange would be composed of land-based, submarine, and aircraft delivered nuclear weapons of the U.S. and U.S.S.R. targeted on military installations, industrial centers, and urban areas. For the purposes of this example of non-local radionuclide effects, we have used the mix of warhead yields and fission yields shown in Table 8.

The application of GLODEP2 models to this type of scenario assumes that if, in fact, there is a "nuclear winter" following the exchange, the effects produce only minor perturbations on the empirically derived deposition models.

U.S.S.R. Weapons		U.S. Weapons	
Yield/Warhead (Mton)	Total Fission Yield Injected (Mton)	Yield/Warhead (Mton)	Total Fission Yield Injected (Mton)
20.	305.	9.	235.
1.	70.	1.-2.	285.
0.9	675.	.3-.4	115.
0.75	15.	.1-.2	105.
0.55	220.	< .1	1.
0.2	5.		
Total Mton injected	1290.		741.

Table 8. Hypothetical Strategic Exchange Scenario (#).

The estimates of available stockpiles used in developing Table 6 are drawn from IISS [25] and Cotter et al. [26]. We have made arbitrary, but plausible, assumptions concerning number of warheads used, fission/fusion fraction, height of burst, etc. It should be recognized that these are hypothetical exchanges and their publication and use does not imply any relationship to the plans of either the United States or the Soviet Union.

We assume that the attack on the U.S. is all injected at 39 degrees North latitude, and that on the U.S.S.R. is injected at 50 degrees North latitude. Of the approximate 2031 Mton of fission products injected, 11% (224 Mton) goes to the troposphere, 61% (1237 Mton) goes to the lower polar stratosphere, and 28% (570 Mton) is placed in the upper polar stratosphere.

In addition to the weapons exchange indicated above, we assume an attack on an approximate 100 GW(e) nuclear power industry in the U.S. We assume 0.9 Mton weapons are surface bursts on 100 LWR's, 100 10-year Spent Fuel storage (SFS) facilities, and 1 Federal Reprocessing Plant (FRP). With a 0.9 Mton burst on each facility, 1.8% of the fission products are injected in the troposphere and 48.2% into the lower polar stratosphere.

The resulting uniform unsheltered, unweathered doses are shown in Table 9. The largest value of 23 rem for the weapons (84.6 for weapons pluse the 100 GW(e) nuclear power industry) is computed in the 30-50 degree North Latitude Band.

If one assumes that the general circulation pattern of the atmosphere remains unchanged due to the strategic interchange, then the GRANTOUR model designed by Walton and MacCracken [26] may be used to compute local "hotspots" due to nuclear debris cloud interactions with storm clouds. Based on such calculations, Knox [18] reports:

> "Depending on season, meteorological conditions during the exchange, and how soon the debris clouds intercept large scale weather systems, the tropospheric portion of the radioactive inventory can be scavenged by precipitation and hotspots of deposited radioactivity can occur with doses of about 70 rem (winter) to 40 to 110 rem (summer) in regions like Europe, western Asia, western North Pacific, southeastern U.S., northeastern U.S., and Canada. Such regional hotspots have been identified by numerical simulation of

interaction of the debris cloud with precipitation systems as depicted in the Oregon State University (OSU) general circulation model."

Inclusion of the effects of an attack on the 100 GW(e) nuclear power industry would indicate similar hotspots, i.e., of the order of 200-300 rem.

As pointed out by Walton [26], these GRANTOUR calculations use a specific sequence of meteorologic events as calculated by the OSU general circulation model. For a different starting time or altered circulation model, which would place precipitation systems differently, results could be very different.

Figure 9 is a contour plot of the fractional deposition. Figure 10 shows the fractional depositions over the 24 quarters for each of the 20 degree latitude bands. In these figures we observe the effects of seasonal rainfall on the deposition. One observes the largest deposition at 30-50N and the smallest, 3-4 orders of magnitude smaller, at 70-90S. Further, no deposition occurs in the southernmost latitude band for the first 6 months after the exchange.

	Latitude Band								
Source	1	2	3	4	5	6	7	8	9
Weapons	3.65	18.	23.	5.7	0.76	0.55	0.78	0.47	0.08
LWR	1.75	6.27	8.94	3.	0.56	0.27	0.25	0.1	0.007
SFS	6.71	23.8	32.7	11.3	2.26	1.01	1.02	0.4	0.03
FRP	4.13	14.6	20.1	7.	1.39	0.62	0.63	0.25	0.02
Total	16.2	62.6	84.6	27.	4.98	2.45	2.67	1.21	0.14

Table 9. Uniform 50-year gamma-ray dose in rem as a function of the 9 latitude bands for the weapons and nuclear power facilities. These values do not take into account any weathering, sheltering or rainfall factors. "Hot-spots" due to rainfall could increase these values by factors of 10-50 [10].

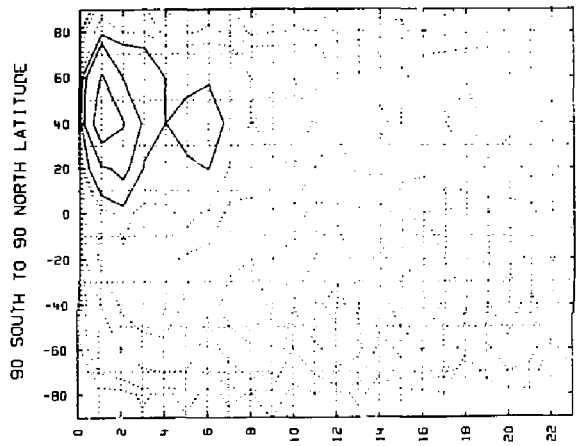

Figure 9. Contour plots of the fractional deposition due to the Strategic Exchange. The abscissa is the time in quarters and the ordinate runs from the South Pole (-90) to the North Pole (+90). The highest solid contour has value 0.1, the next 0.03, then 0.01. The dotted contours are 0.03, 0.001, 0.003, 0.0001 and 0.0003.

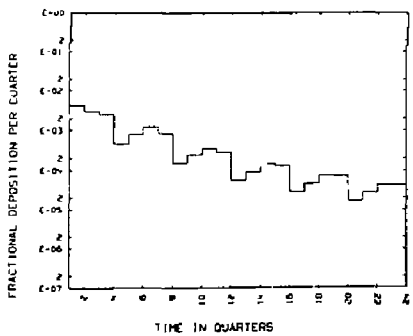

Figure 10a. 70-90N

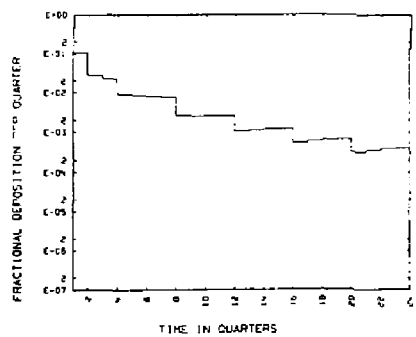

Figure 10b. 50-70N

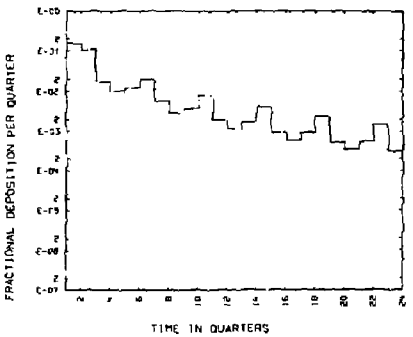

Figure 10c. 30-50N

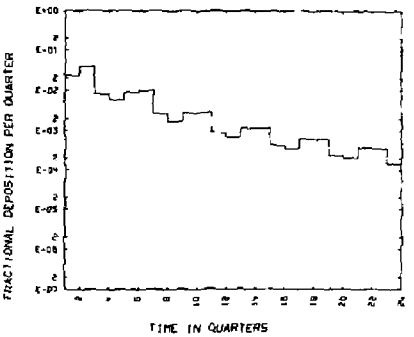

Figure 10d. 10-30N

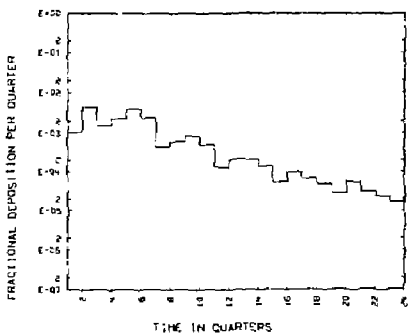

Figure 10e. 10S-10N

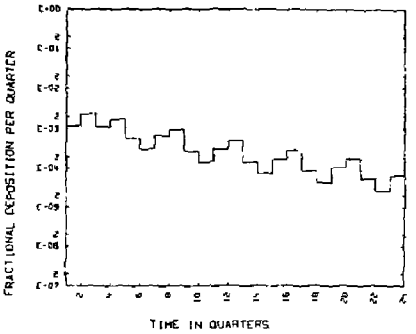

Figure 10f. 10-30S

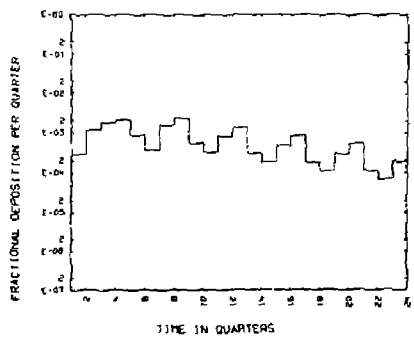

Figure 10g. 30-50S

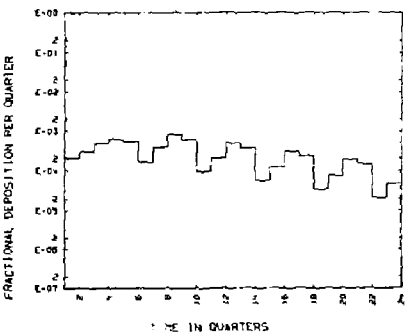

Figure 10h. 50-70S

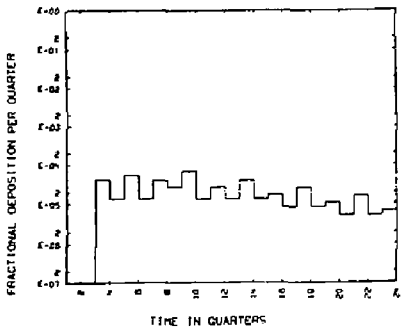

Figure 10i. 70-90S

Figure 10. Fractional depositions as a function of quarters after injection for each of the 20-degree latitude bands.

Figure 11 is a contour plot of the accumulated dose for only the weapons. Figure 12 includes the 110 GW(e) nuclear power industry. One observes the highest dose contour at about 40N. The highest contour for only the weapons appears early in time whereas the highest contour when the nuclear power facilities are included does not appear until about 40 quarters. This effect is due to the rapid decay of weapons fission products compared to the relatively slow decay of the fission products in the 10-year spent fuel waste storage and the federal nuclear waste reprocessing plant. Figure 13 shows the accumulated gamma dose as a function of time for each of the latitude bands. The separation of the two curves at late time also shows the difference of decay rates.

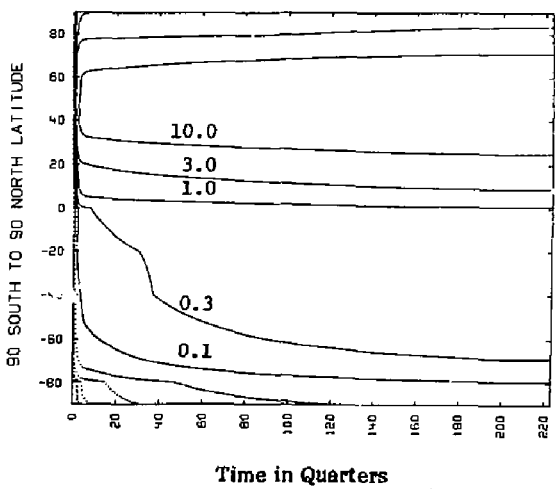

Figure 11. Contour plot of the accumulated gamma dose for only the weapons of the Strategic Exchange. The abscissa is the time in quarters and the ordinate runs from the South Pole (-90) to the North Pole (+90).

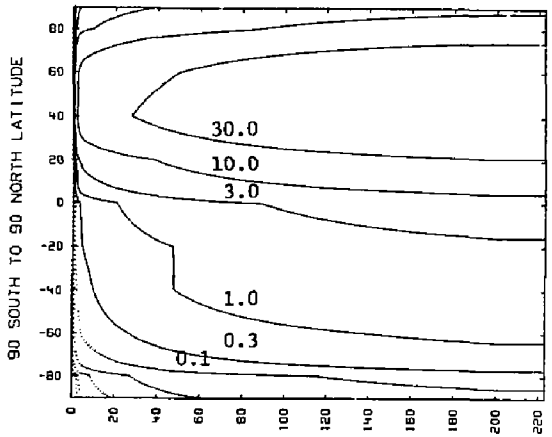

Figure 12. Contour plot of the accumulated gamma dose due to the Strategic Exchange augmented with a 100 GW(e) nuclear power industry. The abscissa is the time in quarters and the ordinate runs from the South Pole (-90) to the North Pole (+90).

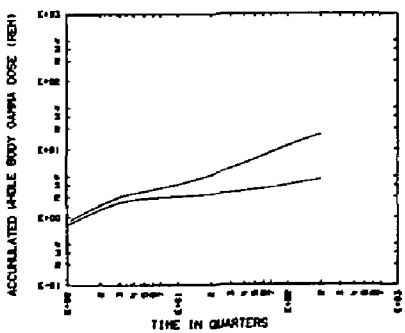

Figure 13a. 70-90N

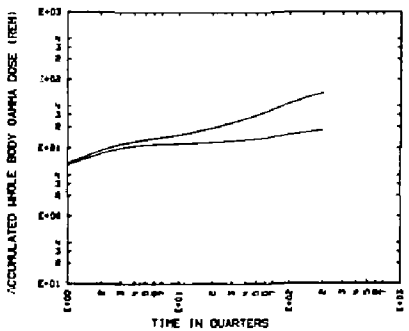

Figure 13b. 50-70N

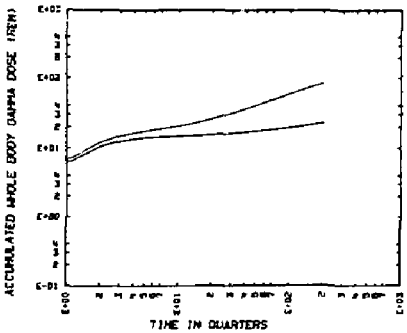

Figure 13c. 30-50N

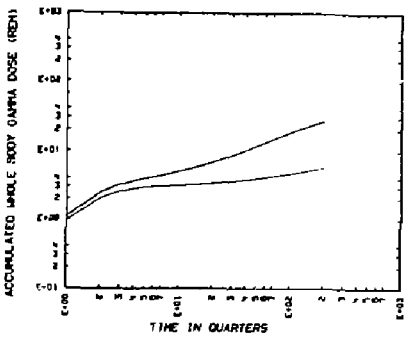

Figure 13d. 10-30N

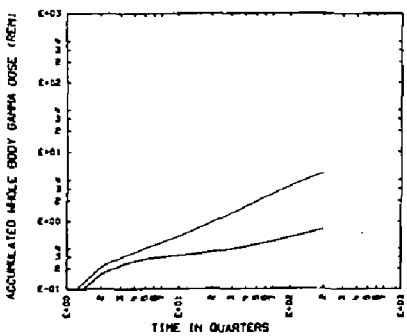

Figure 13e. 10S-10N

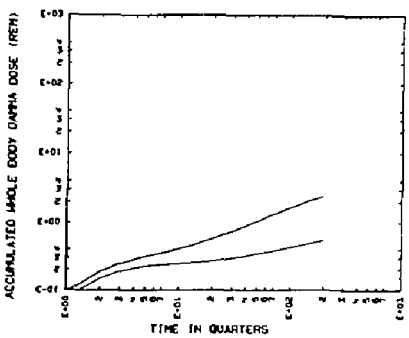

Figure 13f. 10-30S

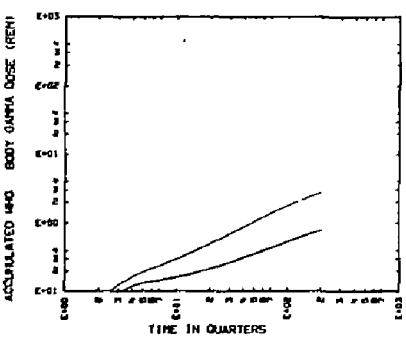

Figure 13g. 30-50S

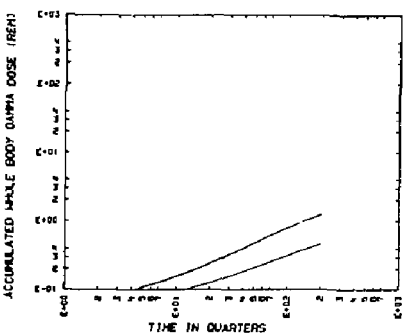

Figure 13h. 50-70S

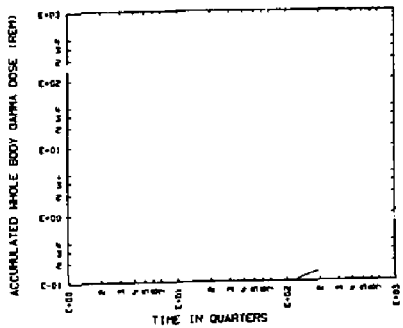

Figure 13i. 70-90S.

Figure 13. Accumulated 50-year gamma dose as a function of quarters for each of the 20-degree latitude bands. The higher value is for the weapons augmented by a 100 GW(e) nuclear power industry.

The dose using the weathering, rainfall, and roughness factor has been computed for five specific locations with results as shown in Table 10.

	London	Montreal	Lisbon	Tokyo	Sydney
Latitude	51.48N	45.57N	38.72N	35.68N	33.87S
Local Average Rainfall (mm)	583	970	701	1560	1200
Latitude Average Rainfall (mm)	819	910	788	733	905
50-yr dose (rem)	17.8	22.3	22.1	27.	0.6

Table 10. Gamma dose in rem for the Strategic Exchange with 100 GW(e) nuclear power facilities at five specific locations.

Figure 14 shows the time dependent accumulation of gamma dose at each of the specific locations with and without the nuclear power facilities augmentation. The effect of weathering on reduction of accumulated dose can be a significant factor. For example, at Tokyo, the interpolated uniform dose would be about 72 rem. With rainfall, penetration, run-off and weathering, the dose is 27 rem after 50 years of accumulation.

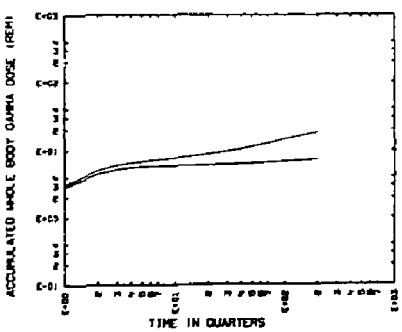

Figure 14a. London

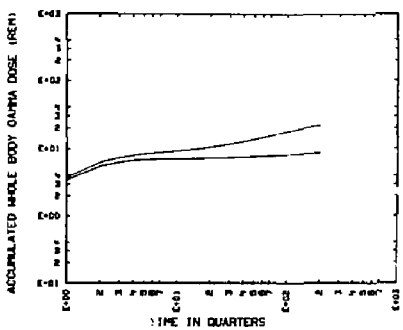

Figure 14b. Montreal

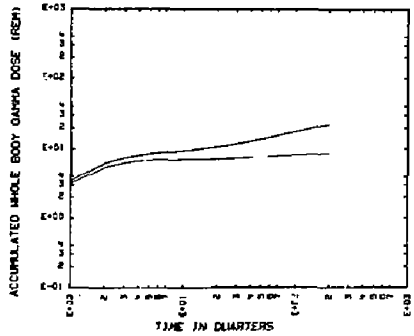

Figure 14c. Lisbon

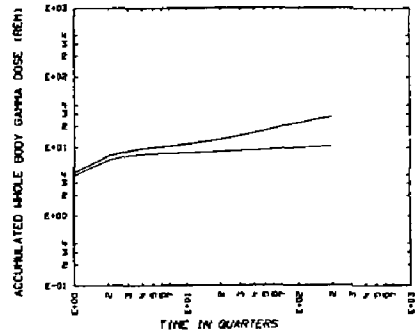

Figure 14d. Tokyo

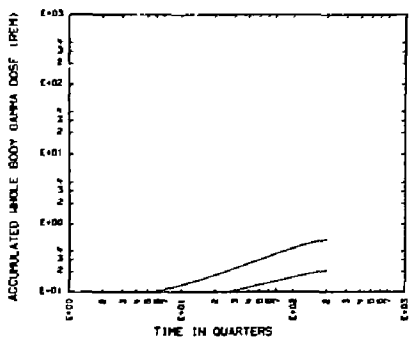

Figure 14e. Sydney

Figure 14. Time accumulated gamma dose using local rainfall, weathering, run-off and a roughness factor for the indicated locations.

5. DISCUSSION AND CONCLUSIONS

The GLODEP2 computer model is capable of estimating the surface deposition of "worldwide" radioactivity and the gamma-ray dose to man from the intermediate and long-term fallout. Code generated predictions of the gamma dose due to the atmospheric tests of 1951-1962 agree well with the measurements at two specific locations.

Although the injection and long-term deposition models of GLODEP2 are only slight modifications of those proposed by Peterson [5], GLODEP2 has original modeling in tropospheric deposition, injection and deposition from nuclear installations, gamma dose, weathering, penetration, runoff, and roughness.

The intermediate term deposition in the Gaussian formulation for fallout from the troposphere appears to be reasonable, in view of the measurements reported by Machta [14]. However, uncertainties exist in terms of the time for completion of fallout as well as the shape of the Gaussian. Further, cross-hemispheric flow is slow, somewhat seasonal and usually occurs in preferred areas. Additional research and modeling is warranted in this area if significant portions of the injections are in the equatorial tropospheric compartment.

The models employed for dose calculations also have margins of uncertainty. The exact values of the dose-area-integrals are unknown for weapons where tests have been conducted. The values for the particular nuclear power facilities have never been tested against an experiment where the facility has been vaporized by a nuclear weapon.

In our models for dose calculations at specific locations we introduce even more margins of uncertainty. The terrain roughness factor of 0.7 may be reasonable for moderately rough terrain. Further research might produce substantial changes in this factor for other regions and certainly for the complexity of urban areas.

The data we have used seem to indicate that the use of the local rain rate/average rain rate to the 3/5ths power may be reasonable; however, we have not used any measurements from areas with little precipitation, nor have we used measurements from areas with tropical or monsoon types of weather.

The penetration-runoff model is based on measurements of ^{137}Cs and applied to the entire inventory of radionuclides. It is well known that the solubility and mobility of other nuclides may vary over wide ranges, hence another area of uncertainty.

Peterson [5] has stated that his "model is based primarily on injection-deposition experience gained from the U.S. and U.S.S.R. nuclear tests in 1958. Use of the technique to estimate ^{90}Sr deposition from the 1961-62 tests shows the predictions are usually within a factor of two of the observed deposition." He further asserts that

> "The comparison of observed and predicted ^{90}Sr deposition...offers one basis for an error analysis. For the 1961-62 tests nearly all seasonal predictions vs. observations agree within a factor of three and most are within a factor of two for 10°N to 70°N and from 10°S to 90°S. From 70°N to 90°N latitude a few seasonal values disagree by a factor of five. From 10°N to 10°S, deviations of a factor of five occur in more than half the seasonal predictions. An independent error analysis, taking into account probable errors in estimates of cloud heights, fission yields, vertical distribution of radioactivity within the cloud, deposition observations and deposition variation for each injection quarter suggests that the discrepancies noted...are typical for a series of bursts such as occurred in 1961-62."

Peterson [5] has also noted the following limitations of the methodology:

> "Because of time and space variations of deposition from individual detonations, deposition predictions for single detonations may be grossly in error. Predictions are for 20° latitude bands and 3-month seasons. Application of these average values to specific locations or shorter times should be made with caution since variations of about an order of magnitude have been observed in 3-month deposition values within 'wet' regions of the United States."

In GLODEP2 we have included models to account for the differences between the "uniform" dose of the 20° latitude bands and that dose at specific locations. Our penetration, run-off and rainfall models are derived primarily from measurements at Grove. However, large portions of these data were obtained from independent, controlled experiments. Further, the injection and deposition models are independent of these data. Thus the computations at Grove and Chiba provide "code validation." We have noted that the values computed for Chiba use the GLODEP2 models directly with no fitting of parameters to the measurements reported there.

In view of the uncertainties associated with the entire suite of GLODEP2 models, the agreement with measurements at the two locations selected may be somewhat fortuitous, but the predictions do lend a measure of credibility to the GLODEP2 model.

It is important to bear in mind that the GLODEP2 deposition models are empirically derived. If a large nuclear exchange were to occur and if, in fact, the exchange caused a "nuclear winter" it is probable that the current empirical circulation and meteorological models would no longer be valid.

Inasmuch as we do not expect to obtain a great deal of new experimental data, sensitivity and uncertainty analyses with the present model are suggested as areas of further research. Future reviews of the existing data coupled with such analyses might lead to some revisions of the models and, more importantly, should lead to predictions that are certainly within acceptable error bounds.

It should be pointed out that even though Peterson [5] suggests a "mirror-image" approach for detonations in the Southern Hemisphere, this technique has not been implemented in the current GLODEP2. Presently we assume all detonations are in the Northern Hemisphere. However, the extension should be a simple programming task.

6. REFERENCES

[1] Smyth, H. D., Method of Assembly, 12, 19, Atomic Energy for Military Purposes, Princeton University Press, (1940), p 212.

[2] AMB'O, A Journal of the Human Environment, vol. XI, Number 2-3 (1982).

[3] Neir, A. O. C., Chairman, Committee to Study the Long-Term Worldwide Effects of Multiple Nuclear-Weapons Detonations, National Academy of Sciences, (Aug. 1975).

[4] Chester, C. V., and R. O. Chester, Civil Defense Implications of the U.S. Nuclear Power Industry During a Large Nuclear War in the Year 2000, Nuclear Technology, vol 31, (Dec. 1976) pp 326-338.

[5] Peterson, K. R., An Empirical Model for Estimating Worldwide Deposition from Atmospheric Nuclear Detonations, Health Phys., Pergamon Press, vol 19, (1970), pp 357-378.

[6] Gale, H. J., D. L. O. Humphreys and E. M. R. Fisher, Weathering of Caesium-137 in Soil, Nature, No. 4916, (Jan. 18, 1964), pp 257-261.

[7] Lowder, W. M., H. L. Beck and W. J. Condon, Dosimetric Investigations of Environmental Gamma Radiation from Deposited Fission Products, Proceedings of the Second Conference on Radioactive Fallout from Nuclear Weapons Tests, U.S.A.E.C., (Nov. 1965).

[8] List, R., L. Salter and K. Telegadas, Tellus 18, 345 (1966).

[9] Ferber, G., Radioactive Fallout from Nuclear Weapons Tests, U.S.A.E.C., Oak Ridge, Tenn. (1965), pp. 629-645.

[10] U.S. Weather Bureau, U.S.A.E.C. Rept HASL-142 (1964), pp. 218-239.

[11] Seitz, H., et al, Final Report on Project Streak: Numerical models of transport, diffusion and fallout of stratospheric radioactive material, Re. NYO-3654-4, Atomic Energy Comm., Washington, D.C., (May 1968).

[12] Telegadas, K., Estimation of Maximum Credible Atmospheric Radioactivity Concentrations and Dose Rates from Nuclear Tests, Atmos. Environ., 13, 327, 1979.

[13] Bauer, E., A Catalog of Perturbing Influences on Stratospheric Ozone, 1955-1975, J. of Geophysical Research, vol 84, No c11, November 20, 1979, pp 6929-6940.

[14] Eisenbud, M., Environmental Radioactivity, 2nd Ed., Academic Press, New York, (1973), p 355.

[15] Glasstone, S., and P. J. Dolan, The Effects of Nuclear Weapons, 3rd Edition, U.S.D.O.D. and U.S.D.O.E. (1977).

[16] Lamb, H. H., Climate: Present, Past and Future, Vol 1, Methuen & Co., LTD, London (1977), p 370.

[17] Harvey, T. F., and L. L. Edwards, Long-Range Nuclear War Fallout Doses Near Selected Non-Combatant Country Cities, UCRL draft report (1983).

[18] Knox, J. B., Global Scale Deposition of Radioactivity from a Large Scale Exchange, Lawrence Livermore National Laboratory Report UCRL-89907 (preprint), (Oct. 1983).

[19] Ionizing Radiation: Sources and Biological Effects, United Nations Scientific Committee on the Effects of Atomic Radiation, 1982 Report to the General Assembly, with annexes, United Nations, New York, (1982).

[20] Gibson, J. A. B., J. E. Richards and J. Docherty, Nuclear Radiation in the Environment-Beta and Gamma-Ray Dose Rates and Air Ionization from 1951 to 1968, J. of Atmospheric and Terrestrial Physics, 31, (1969), pp 1183-1196.

[21] Yamasaki, F., M. Okano, T. Nagahana and H. Watanabe, External Doses of Radiation from Fallout in Tokyo and its Vicinity, J. of Radiation Research, 5, (1964), pp 113-115.

[22] National Institute of Radiological Sciences, Chiba, Japan. External Doses of Radiation from Fallout, Radioactivity Survey Data in Japan, No. 15, (1967), pp 8-9.

[23] National Institute of Radiological Sciences, Chiba, Japan, External Doses of Radiation from Fallout in Tokyo and its Vicinity, Radioactivty Survey Data in Japan, No. 19, (1968), pp 10-11.

[24] Ionizing Radiation: Levels and Effects, Vol. 1, Levels, United Nationals Scientific Committee on the Effects of Atomic Radiation, New York, (1972), p 56.

[25] Cotter, D. R., J. H. Hansen, and K. McConnell, The Nuclear "Balance" in Europe: Status, Trends, Implications, United States Strategic Institute, USSI Report 83-1, 1983).

[26] Walton, J. J. and M. C. MacCracken, Preliminary Report on the Global Transport Model GRANTOUR, Lawrence Livermore National Laboratory, Livermore, CA., UCID-19985 (1984).

0226G

APPENDIX A

The following data tables have been taken from the work of Peterson (1970). In the following we have converted most numbers to pure fractions.

Table A-1a. Fractional injections from equatorial airbursts.
(Fission yield=total yield)

	Total yield (Mton)															
	0.05	0.07	0.1	0.2	0.3	0.5	0.7	1	2	3	5	7	10	20	30	50
Cloud top (km)	17.1	17.4	17.4	18.0	18.3	18.9	19.1	19.8	22.0	23.8	26.5	28.4	30.5	35.4	39.4	42.7
Cloud base (km)	10.4	10.4	10.4	11.0	11.3	11.9	12.1	12.8	14.0	14.9	16.2	17.4	18.3	18.9	20.7	21.3
Mt <17km	0.049	0.068	0.093	0.18	0.26	0.49	0.62	0.85	0.55	0.24	0.02	0	0	0	0	0
Mt 17-24 km	0.001	0.002	0.003	0.02	0.04	0.10	0.18	0.35	1.45	2.78	4.43	4.97	5.25	3.0	2.1	0.5
Mt 24-50 km	0	0	0	0	0	0	0	0	0	0	0.55	2.03	4.75	17.0	27.9	49.5
Mt >50 km	0	0	0	0	0	0	0	0	0	0	0	0	0	0	0	0

Table A-1b. Fractional injections from polar airbursts.
(Fission yield=total yield)

	Total yield (Mton)															
	0.03	0.05	0.07	0.1	0.2	0.3	0.5	0.7	1	2	3	5	7	10	20	30	50
Cloud top (km)	10.1	10.4	10.7	11.0	11.6	12.2	12.4	14.5	16.2	18.5	22.0	25.3	27.7	30.3	34.5	38.1	42.7
Cloud base (km)	4.0	4.3	4.6	4.9	5.5	5.8	6.7	7.3	7.9	9.8	11.0	12.8	13.7	15.5	18.3	19.5	20.7
Mt<9 km	0.029	0.045	0.06	0.08	0.14	0.17	0.16	0.08	0.01	0	0	0	0	0	0	0	0
Mt 9-17 km	0.001	0.003	0.01	0.02	0.06	0.13	0.34	0.62	0.99	1.60	1.45	0.95	0.58	0.46	0	0	0
Mt 17-50 km	0	0	0	0	0	0	0	0	0	0.40	1.55	4.05	6.44	9.04	19.8	30.0	50.0
Mt > 50 km	0	0	0	0	0	0	0	0	0	0	0	0	0	0	0	0	0

Table A-2a. Fractional deposition (x 100) for injection of debris during Dec-Feb into the Lower Equatorial Stratosphere (17-24 km).

	1st yr				2nd yr				3rd yr	
Latitude	Dec-Feb	Mar-May	June-Aug	Sept-Nov	Dec-Feb	Mar-May	June-Aug	Sept-Nov	Dec-Feb	Mar-May
70-90N	.04	.41	.12	.06	.06	.14	.04	.02	.02	.05
50-70N	.52	4.60	1.39	.66	.68	1.60	.49	.23	.24	.56
30-50N	1.12	9.89	3.03	1.42	1.46	3.43	1.07	.50	.52	1.21
10-30N	1.44	2.39	3.10	.74	1.05	1.39	1.09	.26	.37	.49
10S-10N	1.40	3.07	2.39	2.52	.66	1.85	.84	.89	.23	.65
10-30S	.56	3.28	2.58	.99	.33	1.07	.91	.35	.12	.38
30-50S	.78	2.46	1.93	2.13	1.42	.64	.68	.75	.50	.23
50-70S	.40	1.24	.96	1.06	.71	.33	.34	.37	.25	.12
70-90S	0	0	0	.01	0	0	0	0	0	0

Table A-2b. Fractional deposition (x 100) for injection of debris during Mar-May into the Lower Equatorial Stratosphere (17-24 km).

	1st yr				2nd yr				3rd yr	
Latitude	Mar-May	June-Aug	Sept-Nov	Dec-Feb	Mar-May	June-Aug	Sept-Nov	Dec-Feb	Mar-May	June-Aug
70-90N	.06	.19	.22	.09	.26	.06	.08	.03	.09	.02
50-70N	.78	2.19	2.51	1.03	2.88	.72	.89	.36	1.02	.25
30-50N	1.68	4.71	5.41	2.23	6.19	1.56	1.91	.79	2.19	.55
10-30N	2.16	1.14	1.30	1.60	2.51	1.60	.45	.56	.89	.56
10S-10N	2.10	1.46	1.67	.99	3.33	1.24	.59	.35	1.18	.44
10-30S	.84	1.56	1.79	.50	1.93	1.33	.63	.18	.68	.47
30-50S	1.17	1.17	1.35	2.15	1.14	1.00	.48	.76	.40	.35
50-70S	.60	.59	.63	1.09	.57	.50	.24	.38	.20	.18
70-90S	0	0	0	.01	0	0	0	0	0	0

Table A-2c. Fractional deposition (x 100) for injection of debris during Jun-Aug into the Lower Equatorial Stratosphere (17-24 km).

	1st yr				2nd yr				3rd yr	
Latitude	June-Aug	Sept-Nov	Dec-Feb	Mar-May	June-Aug	Sept-Nov	Dec-Feb	Mar-May	June-Aug	Sept-Nov
70-90N	.02	.21	.15	.32	.07	.05	.05	.11	.03	.02
50-70N	.26	2.37	1.64	3.48	.81	.56	.58	1.23	.29	.20
30-50N	.56	5.10	3.54	7.48	1.76	1.21	1.25	2.64	.62	.43
10-30N	.72	1.23	2.54	3.04	1.80	.63	.90	1.07	.64	.22
10S-10N	.70	1.58	1.57	4.03	1.39	2.15	.56	1.42	.49	.76
10-30S	.28	1.69	.79	2.33	1.50	.85	.28	.82	.53	.30
30-50S	.39	1.27	3.42	1.38	1.12	1.82	1.21	.49	.40	.64
50-70S	.20	.64	1.73	.69	.56	.91	.61	.25	.20	.32
70-90S	0	0	.02	0	[illegible]	.01	0	0	0	0

Table A-2d. Fractional deposition (x 100) for injection of debris during Sep-Nov into the Lower Equatorial Stratosphere (17-24 km).

	1st yr				2nd yr				3rd yr	
Latitude	Sept-Nov	Dec-Feb	Mar-May	June-Aug	Sept-Nov	Dec-Feb	Mar-May	June-Aug	Sept-Nov	Dec-Feb
70-90N	.03	.22	.37	.09	.05	.05	.13	.03	.02	.02
50-70N	.39	2.51	4.04	1.04	.60	.63	1.43	.37	.21	.22
30-50N	.84	5.41	8.68	2.25	1.31	1.35	3.06	.79	.46	.48
10-30N	1.08	1.30	3.53	2.30	.68	.97	1.25	.81	.24	.34
10S-10N	1.05	1.67	4.67	1.78	2.32	.60	1.65	.63	.82	.21
10-30S	.42	1.79	2.70	1.92	.92	.30	.95	.68	.32	.11
30-50S	.59	1.35	1.60	1.43	1.97	1.31	.56	.50	.70	.46
50-70S	.30	.68	.80	.72	.98	.66	.28	.25	.35	.23
70-90S	0	0	0	0	.01	0	0	0	0	0

Table A-3a. Fractional deposition (x 100) for injection of debris during Dec-Feb into the Upper Equatorial Stratosphere (24-50 km).

	1st yr				2nd yr				3rd yr				4th yr
Latitude	Dec-Feb	Mar-May	June-Aug	Sept-Nov	Dec-Feb	Mar-May	June-Aug	Sept-Nov	Dec-Feb	Mar-May	June-Aug	Sept-Nov	Dec-Feb
70-90N	0	.04	.03	.03	.04	.14	.05	.03	.03	.10	.04	.02	.02
50-70N	0	.46	.33	.28	.46	1.60	.58	.33	.40	1.12	.41	.23	.28
30-50N	0	.99	.72	.60	.98	3.43	1.27	.71	.87	2.42	.90	.50	.62
10-30N	0	.24	.59	.32	.71	1.39	1.29	.37	.62	.98	.91	.26	.44
10S-10N	0	.27	.44	.47	.48	.97	.90	.49	.40	.69	.64	.35	.28
10-30S	0	.11	.53	1.14	.67	.56	.95	1.34	.74	.39	.67	.95	.52
30-50S	0	.45	.74	2.80	.74	1.07	1.31	3.30	.78	.76	.93	2.33	.55
50-70S	0	.21	.34	1.30	.48	.49	.61	1.54	.43	.35	.43	1.09	.30
70-90S	0	.02	.03	.12	.04	.04	.05	.14	.04	.04	.04	.10	.03

Table A-3b. Fractional deposition (x 100) for injection of debris during Mar-May into the Upper Equatorial Stratosphere (24-50 km).

	1st yr				2nd yr				3rd yr				4th yr
Latitude	Mar-May	June-Aug	Sept-Nov	Dec-Feb	Mar-May	June-Aug	Sept-Nov	Dec-Feb	Mar-May	June-Aug	Sept-Nov	Dec-Feb	Mar-May
70-90N	0	.02	.04	.03	.13	.04	.07	.03	.11	.03	.05	.02	.08
50-70N	0	.16	.45	.33	1.46	.54	.80	.38	1.29	.38	.57	.27	.91
30-50N	0	.35	.96	.71	3.13	1.17	1.71	.84	2.77	.82	1.21	.59	1.96
10-30N	0	.09	.23	.51	1.27	1.20	.41	.60	1.12	.84	.29	.42	.79
10S-10N	0	.13	.40	.42	.64	.84	.54	.49	.56	.60	.39	.35	.40
10-30S	0	.12	.79	.92	.43	.92	1.41	1.09	.38	.64	1.00	.77	.27
30-50S	0	.51	1.95	.90	.84	1.28	3.45	1.06	.73	.91	2.44	.75	.52
50-70S	0	.24	.91	.42	.38	.60	1.61	.50	.33	.42	1.14	.35	.23
70-90S	0	.02	.08	.04	.03	.05	.15	.04	.03	.04	.11	.03	.02

Table A-3c. Fractional deposition (x 100) for injection of debris during Jun-Aug into the Upper Equatorial Stratosphere (24-50 km).

Latitude	1st yr June-Aug	1st yr Sept-Nov	1st yr Dec-Feb	1st yr Mar-May	2nd yr June-Aug	2nd yr Sept-Nov	2nd yr Dec-Feb	2nd yr Mar-May	3rd yr June-Aug	3rd yr Sept-Nov	3rd yr Dec-Feb	3rd yr Mar-May	4th yr June-Aug
70-90N	0	.02	.03	.12	.04	.04	.05	.14	.04	.04	.04	.10	.03
50-70N	0	.21	.34	1.30	.48	.49	.61	1.54	.43	.35	.43	1.09	.30
30-50N	0	.45	.74	2.80	.74	1.07	1.31	3.30	.78	.76	.93	2.33	.55
10-30N	0	.11	.53	1.14	.67	.56	.95	1.34	.74	.39	.67	.95	.52
10S-10N	0	.23	.40	.63	.51	.83	.80	.62	.40	.59	.57	.44	.28
10-30S	0	.24	.59	.32	.71	1.39	1.29	.37	.62	.98	.91	.26	.44
30-50S	0	.99	.72	.60	.98	3.43	1.27	.71	.87	2.42	.90	.50	.62
50-70S	0	.46	.33	.28	.46	1.60	.58	.33	.40	1.12	.41	.23	.28
70-90S	0	.04	.03	.03	.04	.14	.05	.03	.03	.10	.04	.02	.02

Table A-3d. Fractional deposition (x 100) for injection of debris during Sep-Nov into the Upper Equatorial Stratosphere (24-50 km).

Latitude	1st yr Sept-Nov	1st yr Dec-Feb	1st yr Mar-May	1st yr June-Aug	2nd yr Sept-Nov	2nd yr Dec-Feb	2nd yr Mar-May	2nd yr June-Aug	3rd yr Sept-Nov	3rd yr Dec-Feb	3rd yr Mar-May	3rd yr June-Aug	4th yr Sept-Nov
70-90N	0	.02	.08	.04	.03	.05	.15	.04	.03	.04	.11	.03	.02
50-70N	0	.24	.91	.42	.38	.60	1.61	.50	.33	.42	1.14	.35	.23
30-50N	0	.51	1.95	.90	.84	1.28	3.45	1.06	.73	.91	2.44	.75	.52
10-30N	0	.12	.79	.92	.43	.92	1.41	1.09	.38	.64	1.00	.77	.27
10S-10N	0	.14	.49	.52	.64	.75	.76	.61	.56	.53	.54	.43	.40
10-30S	0	.09	.23	.51	1.27	1.20	.41	.60	1.12	.84	.29	.42	.79
30-50S	0	.35	.96	.71	3.13	1.17	1.71	.84	2.77	.82	1.21	.59	1.96
50-70S	0	.16	.45	.33	1.46	.54	.80	.38	1.29	.38	.57	.27	.91
70-90S	0	.02	.04	.03	.13	.04	.07	.03	.11	.03	.05	.02	.08

Table A-4a. Fractional deposition (x 100) for injection of debris during Mar-Aug into the High Equatorial Atmospher (above 50 km).

Latitude	1st yr Mar-May	1st yr June-Aug	1st yr Sept-Nov	1st yr Dec-Feb	2nd yr Mar-May	2nd yr June-Aug	2nd yr Sept-Nov	2nd yr Dec-Feb	3rd yr Mar-May	3rd yr June-Aug	3rd yr Sept-Nov	3rd yr Dec-Feb	4th yr Mar-May	4th yr June-Aug	4th yr Sept-Nov	4th yr Dec-Feb	5th yr Mar-May	5th yr June-Aug	5th yr Sept-Nov	5th yr Dec-Feb	6th yr Mar-May	6th yr June-Aug	6th yr Sept-Nov	6th yr Dec-Feb
70-90N	0	0	0	0	0	0	0	.01	.01	.04	.01	.02	.03	.08	.01	.01	.02	.05	.01	.01	.01	.03	.01	.01
50-70N	0	0	0	0	0	0	0	.03	.26	.36	.17	.32	.87	.71	.21	.20	.55	.45	.13	.13	.35	.29	.09	.08
30-50N	0	0	0	0	0	0	0	.12	.71	.28	.18	1.20	2.37	.56	.23	.76	1.49	.35	.14	.48	.94	.22	.09	.30
10-30N	0	0	0	0	0	0	0	.05	.24	.13	.10	.43	.81	.25	.13	.27	.51	.16	.08	.17	.32	.10	.05	.11
10S-10N	0	0	0	0	0	0	0	.01	.04	.05	.08	.11	.12	.09	.10	.07	.08	.08	.06	.04	.05	.04	.04	.03
10-30S	0	0	0	0	0	.14	.51	.31	.29	1.37	2.54	.79	.41	.86	1.60	.50	.26	.54	1.01	.31	.17	.34	.64	.20
30-50S	0	0	0	0	0	.39	1.50	.70	.50	3.80	7.47	1.76	.71	2.40	4.70	1.10	.46	1.51	2.97	.70	.29	.96	1.87	.44
50-70S	0	0	0	0	0	.10	.56	.00	.47	1.00	2.76	2.26	.67	.63	1.74	1.43	.43	.40	1.10	.90	.27	.28	.70	.57
70-90S	0	0	0	0	0	.01	.01	.10	.03	.08	.09	.26	.04	.05	.06	.16	.03	.03	.03	.10	.01	.01	.01	.06

Table A-4b. Fractional deposition (x 100) for injection of debris during Sep-Feb into the High Equatorial Atmosphere (above 50 km).

Latitude	1st yr Sept-Nov	1st yr Dec-Feb	1st yr Mar-May	1st yr June-Aug	2nd yr Sept-Nov	2nd yr Dec-Feb	2nd yr Mar-May	2nd yr June-Aug	3rd yr Sept-Nov	3rd yr Dec-Feb	3rd yr Mar-May	4th yr June-Aug	4th yr Sept-Nov	4th yr Dec-Feb	4th yr Mar-May	5th yr June-Aug	5th yr Sept-Nov	5th yr Dec-Feb	5th yr Mar-May	6th yr June-Aug	6th yr Sept-Nov	6th yr Dec-Feb	6th yr Mar-May	6th yr June-Aug
70-90N	0	0	0	0	0	.01	.01	.10	.03	.08	.09	.26	.04	.05	.06	.16	.03	.03	.03	.10	.01	.01	.01	.06
50-70N	0	0	0	0	0	.10	.56	.90	.47	1.00	2.76	2.26	.67	.63	1.74	1.43	.43	.40	1.10	.90	.27	.28	.70	.57
30-50N	0	0	0	0	0	.39	1.50	.70	.50	3.80	7.47	1.76	.71	2.40	4.70	1.10	.46	1.51	2.97	.70	.29	.96	1.87	.44
10-30N	0	0	0	0	0	.14	.51	.31	.29	1.37	2.54	.79	.41	.86	1.60	.50	.26	.54	1.01	.31	.17	.34	.64	.20
10S-10N	0	0	0	0	0	0	0	.01	.04	.05	.08	.11	.12	.09	.10	.07	.08	.06	.06	.04	.05	.04	.04	.03
10-30S	0	0	0	0	0	0	0	.05	.24	.13	.10	.43	.81	.25	.13	.27	.51	.16	.08	.17	.32	.10	.05	.11
30-50S	0	0	0	0	0	0	0	.12	.71	.28	.18	1.20	2.37	.56	.23	.76	1.49	.35	.14	.48	.94	.22	.09	.30
50-70S	0	0	0	0	0	0	0	.03	.26	.36	.17	.32	.87	.71	.21	.20	.55	.45	.13	.13	.35	.29	.09	.08
70-90S	0	0	0	0	0	0	0	.01	.01	.04	.01	.02	.03	.08	.01	.01	.02	.05	.01	.01	.01	.03	.01	.01

Table A-5a. Fractional deposition (x 100) for injection of debris during Dec-Feb into the Lower Polar Stratosphere (9-17 km).

	1st yr				2nd yr			
Latitude	Dec-Feb	Mar-May	June-Aug	Sept-Nov	Dec-Feb	Mar-May	June-Aug	Sept-Nov
70-90N	.27	.69	.54	.09	.15	.23	.13	.02
50-70N	2.86	6.60	5.11	1.80	1.50	1.35	1.21	.34
30-50N	4.94	25.03	8.99	2.00	2.15	2.59	.94	.38
10-30N	1.52	9.17	1.83	1.20	1.62	1.91	.43	.23
10S-10N	.23	1.06	.35	.51	.92	.56	.08	.10
10-30S	.29	.55	.25	.33	.10	.05	.06	.06
30-50S	.07	.27	.43	.29	.12	.05	.10	.05
50-70S	.05	.07	.10	.07	.02	.02	.02	.01
70-90S	0	0	.01	0	0	0	0	0

Table A-5b. Fractional deposition (x 100) for injection of debris during Mar-May into the Lower Polar Stratosphere (9-17 km).

	1st yr				2nd yr			
Latitude	Mar-May	June-Aug	Sept-Nov	Dec-Feb	Mar-May	June-Aug	Sept-Nov	Dec-Feb
70-90N	.43	.19	.22	.20	.18	.27	.04	.03
50-70N	4.46	1.85	2.50	3.97	5.51	2.56	.47	.75
30-50N	7.72	7.00	5.00	7.74	15.01	1.99	.95	1.46
10-30N	2.38	2.15	2.00	3.50	5.11	.91	.38	.66
10S-10N	.35	.30	.60	.30	.46	.18	.11	.06
10-30S	.20	.16	.30	.23	.10	.13	.06	.04
30-50S	.05	.08	.52	.20	.15	.11	.14	.04
50-70S	.07	.02	.17	.07	.14	.05	.03	.01
70-90S	0	0	.01	0	0	0	0	0

Table A-5c. Fractional deposition (x 100) for injection of debris during Jun-Aug into the Lower Polar Stratosphere (9-17 km).

	1st yr				2nd yr			
Latitude	June-Aug	Sept-Nov	Dec-Feb	Mar-May	June-Aug	Sept-Nov	Dec-Feb	Mar-May
70-90N	.18	.19	.18	.21	.38	.03	.04	.04
50-70N	1.89	1.79	3.43	6.42	3.58	.63	.91	1.21
30-50N	3.26	6.79	12.99	17.51	2.79	.70	.97	3.31
10-30N	1.01	2.49	4.76	5.96	1.28	.42	.65	1.13
10S-10N	.15	.29	.55	.53	.25	.18	.37	.10
10-30S	.19	.15	.29	.11	.18	.12	.04	.02
30-50S	.05	.07	.14	.34	.30	.10	.05	.06
50-70S	.03	.02	.03	.16	.07	.02	.01	.01
70-90S	0	0	0	.01	.01	0	0	0

Table A-5d. Fractional deposition (x 100) for injection of debris during Sep-Nov into the Lower Polar Stratosphere (9-17 km).

	1st yr				2nd yr			
Latitude	Sept-Nov	Dec-Feb	Mar-May	June-Aug	Sept-Nov	Dec-Feb	Mar-May	June-Aug
70-90N	.23	.21	.24	.43	.04	.07	.10	.06
50-70N	2.40	3.93	7.34	4.09	.81	.70	.58	.30
30-50N	4.15	14.90	20.01	3.19	.90	1.00	1.11	.28
10-30N	1.28	5.46	6.81	1.46	.54	.78	.82	.25
10S-10N	.19	.63	.61	.28	.23	.44	.24	.05
10-30S	.24	.33	.13	.20	.15	.05	.02	.01
30-50S	.06	.16	.39	.34	.13	.06	.02	.01
50-70S	.04	.04	.18	.08	.03	.01	.01	.01
70-90S	0	0	.01	.01	0	0	0	0

Table A-6a. Fractional deposition (x 100) for injection of debris during Dec-Feb into the Upper Polar Stratosphere (17-50 km).

	1st yr				2nd yr				3rd yr				4th yr	
Latitude	Dec-Feb	Mar-May	June-Aug	Sept-Nov	Dec-Feb	Mar-May	June-Aug	Sept-Nov	Dec-Feb	Mar-May	June-Aug	Sept-Nov	Dec-Feb	Mar May
70-90N	.02	.06	.16	.06	.13	.19	.20	.05	.09	.12	.13	.03	.05	.08
50-70N	.07	.58	1.50	1.14	1.50	1.81	1.89	.90	1.00	1.14	1.19	.57	.65	.72
30-50N	.20	2.18	1.18	1.27	2.58	6.88	1.48	1.00	1.63	4.33	.93	.63	1.02	2.73
10-30N	.05	.52	.54	.76	1.74	1.66	.68	.60	1.09	1.04	.43	.38	.69	.66
10S-10N	0	.03	.05	.17	.10	.10	.09	.15	.08	.06	.05	.10	.05	.04
10-30S	0	.01	.06	.23	.12	.08	.32	.53	.15	.08	.20	.34	.10	.05
30-50S	0	.02	.02	.66	.27	.11	.86	1.57	.34	.21	.55	.99	.21	.13
50-70S	0	0	.05	.24	.34	.06	.23	.58	.43	.06	.14	.36	.27	.04
70-90S	0	0	0	.01	.04	.01	.03	.02	.05	.01	.02	.01	.03	.01

Table A-6b. Fractional deposition (x 100) for injection of debris during Mar-May into the Upper Polar Stratosphere (17-50 km).

	1st yr				2nd yr				3rd yr				4th yr	
Latitude	Mar-May	June-Aug	Sept-Nov	Dec-Feb	Mar-May	June-Aug	Sept-Nov	Dec-Feb	Mar-May	June-Aug	Sept-Nov	Dec-Feb	Mar-May	June-Aug
70-90N	.08	.01	.04	.10	.13	.04	.06	.07	.08	.02	.04	.04	.05	.01
50-70N	.14	.11	.51	1.74	4.07	.35	.64	1.37	2.56	.22	.40	.86	1.61	.14
30-50N	.30	.42	1.01	3.39	11.08	1.33	1.28	2.67	6.98	.83	.80	1.68	4.40	.52
10-30N	.08	.13	.41	1.91	3.77	.41	.51	1.21	2.38	.26	.32	.76	1.50	.16
10S-10N	0	.01	.07	.08	.18	.04	.11	.07	.13	.03	.07	.04	.08	.02
10-30S	0	.02	.11	.07	.07	.23	.57	.17	.08	.21	.36	.10	.05	.13
30-50S	0	.06	.33	.15	.11	.61	1.67	.36	.14	.58	1.05	.23	.09	.37
50-70S	0	.01	.12	.19	.10	.16	.61	.46	.12	.15	.39	.29	.08	.09
70-90S	0	0	0	.02	.01	.02	.02	.05	.01	.02	.01	.03	0	.01

Table A-6c. Fractional deposition (x 100) for injection of debris during Jun-Aug into the Upper Polar Stratosphere (17-50 km).

Latitude	1st yr June-Aug	1st yr Sept-Nov	1st yr Dec-Feb	1st yr Mar-May	2nd yr June-Aug	2nd yr Sept-Nov	2nd yr Dec-Feb	2nd yr Mar-May	3rd yr June-Aug	3rd yr Sept-Nov	3rd yr Dec-Feb	3rd yr Mar May	4th yr June-Aug	4th yr Sept-Nov
70-90N	.01	.01	.07	.09	.28	.04	.06	.07	.18	.02	.04	.05	.11	.01
50-70N	.04	.11	.70	2.84	2.67	.34	.88	2.23	1.68	.22	.56	1.41	1.06	.14
30-50N	.15	.41	2.66	7.73	2.08	1.30	3.35	6.09	1.31	.82	2.11	3.83	.82	.52
10-30N	.03	.15	.97	2.63	.95	.47	1.23	2.07	.60	.30	.77	1.31	.38	.19
10S-10N	0	.01	.06	.13	.11	.05	.09	.13	.08	.04	.04	.08	.05	.03
10-30S	0	.03	.04	.07	.24	.31	.19	.17	.30	.29	.12	.10	.19	.18
30-50S	0	.12	.08	.12	.36	1.27	.41	.28	.45	1.20	.26	.17	.28	.76
50-70S	0	.03	.10	.11	.33	.33	.52	.25	.42	.32	.33	.16	.27	.20
70-90S	0	0	.01	.01	.06	.04	.06	.01	.10	.03	.04	.01	.05	.02

Table A-6d. Fractional deposition (x 100) for injection of debris during Sep-Nov into the Upper Polar Stratosphere (17-50 km).

Latitude	1st yr Sept-Nov	1st yr Dec-Feb	1st yr Mar-May	2nd yr June-Aug	2nd yr Sept-Nov	2nd yr Dec-Feb	2nd yr Mar-May	3rd yr June-Aug	3rd yr Sept-Nov	3rd yr Dec-Feb	3rd yr Mar-May	4th yr June-Aug	4th yr Sept-Nov	4th yr Dec-Feb
70-90N	.02	.03	.06	.23	.04	.06	.08	.18	.02	.04	.05	.12	.01	.02
50-70N	.06	.29	1.84	2.22	.74	.92	2.32	1.74	.47	.58	1.46	1.10	.29	.37
30-50N	.17	1.11	5.02	1.73	.82	3.50	6.33	1.36	.52	2.20	3.99	.86	.33	1.39
10-30N	.04	.41	1.71	.79	.50	1.28	2.15	.62	.31	.81	1.36	.39	.20	.51
10S-10N	0	.02	.08	.08	.12	.07	.12	.07	.10	.05	.07	.05	.06	.03
10-30S	0	.01	.02	.13	.48	.07	.13	.31	.61	.07	.08	.19	.38	.04
30-50S	0	.02	.07	.29	1.41	.23	.33	.68	1.78	.21	.21	.43	1.12	.13
50-70S	0	.01	.03	.15	.52	.06	.16	.35	.65	.06	.10	.22	.41	.04
70-90S	0	0	0	.01	.02	.01	.02	.03	.02	.01	.01	.02	.01	.01

Table A-7a. Fractional deposition (x 100) for injection of debris during Mar-Aug into the High Polar Atmosphere (above 50 km).

Latitude	1st yr Mar-May	1st yr June-Aug	1st yr Sept-Nov	1st yr Dec-Feb	2nd yr Mar-May	2nd yr June-Aug	2nd yr Sept-Nov	3rd yr Dec-Feb	3rd yr Mar-May	3rd yr June-Aug	3rd yr Sept-Nov	4th yr Dec-Feb	4th yr Mar-May	4th yr June-Aug	4th yr Sept-Nov	5th yr Dec-Feb	5th yr Mar-May	5th yr June-Aug	5th yr Sept-Nov	6th yr Dec-Feb	6th yr Mar-May	6th yr June-Aug	6th yr Sept-Nov	Dec-Feb
70-90N	0	0	0	0	0	0	0	.01	.03	.09	.03	.05	.07	.19	.03	.04	.04	.12	.01	.02	.03	.08	.01	.02
50-70N	0	0	0	0	0	0	0	.08	.61	.84	.40	.74	2.03	1.66	.49	.47	1.28	1.05	.31	.29	.81	.67	.20	.19
30-50N	0	0	0	0	0	0	0	.28	1.65	.65	.43	2.81	5.52	1.30	.53	1.77	3.47	.82	.33	1.12	2.19	.52	.21	.70
10-30N	0	0	0	0	0	0	0	.11	.56	.29	.24	1.01	1.88	.59	.31	.64	1.18	.37	.19	.40	.74	.23	.12	.25
10S-10N	0	0	0	0	0	0	0	.01	.04	.05	.08	.11	.12	.09	.10	.07	.08	.06	.06	.04	.05	.04	.04	.03
10-30S	0	0	0	0	0	.07	.24	.15	.13	.64	1.19	.37	.19	.40	.75	.23	.12	.25	.47	.15	.08	.16	.30	.09
30-50S	0	0	0	0	0	.18	.70	.33	.23	1.77	3.49	.82	.33	1.12	2.19	.51	.21	.71	1.39	.33	.13	.45	.87	.21
50-70S	0	0	0	0	0	.05	.26	.42	.22	.47	1.29	1.05	.31	.28	.81	.67	.20	.19	.51	.42	.13	.12	.33	.27
70-90S	0	0	0	0	0	.01	.01	.05	.01	.04	.04	.12	.02	.03	.03	.07	.01	.01	.01	.05	.01	.01	.01	.03

Table A-7b. Fractional deposition (x 100) for injection of debris during Sep-Feb into the High Polar Atmosphere (above 50 km).

Latitude	1st yr Sept-Nov	1st yr Dec-Feb	1st yr Mar-May	1st yr June-Aug	2nd yr Sept-Nov	2nd yr Dec-Feb	2nd yr Mar-May	3rd yr June-Aug	3rd yr Sept-Nov	3rd yr Dec-Feb	3rd yr Mar-May	4th yr June-Aug	4th yr Sept-Nov	4th yr Dec-Feb	4th yr Mar-May	5th yr June-Aug	5th yr Sept-Nov	5th yr Dec-Feb	5th yr Mar-May	6th yr June-Aug	6th yr Sept-Nov	6th yr Dec-Feb	6th yr Mar-May	June-Aug
70-90N	0	0	0	0	0	.01	.01	.09	.03	.06	.08	.24	.04	.04	.05	.15	.03	.03	.03	.09	.01	.01	.01	.05
50-70N	0	0	0	0	0	.09	.52	.84	.44	.93	2.57	2.10	.63	.59	1.62	1.33	.40	.37	1.02	.84	.25	.24	.65	.53
30-50N	0	0	0	0	0	.36	1.40	.65	.47	3.54	6.96	1.64	.67	2.23	4.38	1.02	.43	1.41	2.77	.65	.27	.89	1.74	.41
10-30N	0	0	0	0	0	.13	.48	.29	.27	1.28	2.37	.73	.39	.80	1.49	.47	.24	.51	.94	.29	.16	.32	.60	.19
10S-10N	0	0	0	0	0	0	0	.01	.04	.05	.08	.11	.12	.09	.10	.07	.08	.06	.06	.04	.05	.04	.04	.03
10-30S	0	0	0	0	0	0	0	.05	.28	.15	.12	.51	.94	.29	.15	.32	.59	.19	.09	.20	.37	.11	.08	.13
30-50S	0	0	0	0	0	0	0	.14	.83	.33	.21	1.41	2.77	.65	.27	.89	1.74	.41	.17	.56	1.10	.26	.11	.35
50-70S	0	0	0	0	0	0	0	.04	.31	.42	.20	.37	1.02	.83	.25	.23	.64	.53	.15	.15	.41	.33	.10	.09
70-90S	0	0	0	0	0	0	0	.01	.01	.05	.01	.02	.03	.09	.01	.02	.02	.06	.01	.01	.01	.04	.01	.01

As noted in Peterson (1970), to extend the deposition tables beyond the tabulated values, multiply the last seasonal entries by the following factors to obtain values 1 year later:

Table	Factor
2a-d	0.35
3a-d	0.71
4a-b	0.63
5a-d	0.19
6a-d	0.63
7a-b	0.63

APPENDIX B (GLODEP2 USERS GUIDE)

A CRAY-1 controllee, GLODEP2, is a CIVIC compilation and load of the LRLTRAN souce file glodep2a. The FORTLIB and TV8OCRAY libraries are used in the loader.

The controllee is executed by typing

glodep2 / time value

and then the user will be asked if input is from file or tty. If from tty, the code operates in a conversational mode asking for input when required.

If the user specifies that the input is from a file, then the code asks for the disk file name. The input file may be created using the TRIX routines and is described below.

If file input, then the deck is made up of lines:

---

nloc rough

---

format (12,f5.2)

nloc-nr of specific locations for dose, ≤ 5
rough is roughness factor (=0.7 from Glasstone)

---

h1 lat1 rain1 h2 lat2 rain2 h3 lat3 rain3 h4 lat4 rain4 h5 lat5 rain5

---

format (5(1x,a1,f5.2,f8.2))

hi=n or s for Northern or Southern Hemisphere, i=1,2,...,nloc
lati=degrees of latitude, $0. \leq$ lati $\leq 90.$ i=1,2,...,nloc
raini=average rainfall, mm/yr, i=1,2,...,nloc

---

nqstart nqexp tropst lplf lpld lcnf land jwl

---

format (i6, 1x, i6,e10.2,5(1x,i1))

nqstart is qtr to start dose exposure (.g≥0)
nqexp is nr of qtrs for dose exposure (.g≥0)
tropst is fraction of quarter for troposphere deposition
lplf=1 if plot latitude deposition fractions, =0 otherwise
lpld=1 if plot latitude doses, =0 otherwise
lcnf=1 if plot deposition fraction contours, =0 otherwise
lcnd=1 if plot dose contours, =0 otherwise
jwl=1 if -1.2 weapons decay law
jwl=2 if 1-Mton decay curve from Chester & Chester

---

yminf ymaxf

---

format (2(1x,e9.2))
this card is read only if lplf=1
If you wish to scale the plot, input ymin and ymax
If you wish to plot to be self-scaled, input both values as zero

---

xmind xmaxd ymind ymaxd

---

format (4(1x,e9.2))
this card is read only if lpld=1
If you wish to scale the plot, input xmin, xmax, ymin and ymax
If you wish the plot to be self-scaled, input all values as zero

---

nqtrf nentrf nqtrppf

---

format (3i5)
this card is read only if lcnf=1
nqtrf is the number of quarters for each contour plot
nentrf is the number of contours to plot (≤ 25)
nqtrppf is the number of quarters for each frame of plot

---

nqtrd ncntrd nqtrppd

---

format (3i5)
this card is read only if lcnd=1
nqtrd is the number of quarters for each contour plot
ncntrd is the number of contours to plot ($\leq$ 25)
nqtrppd is the number of quarters for each frame of plot

---

nqs iyears

---

format (i1,1x,i4)
nqs is the start quarter for first injection
=1 for Dec-Feb
=2 for Mar-May
=3 for Jun-Aug
=4 for Sep-Nov
iyears is the calendar year to start injection, e.g. 1985 or 2000

---

ntest ty ff hob nf nnf detl

---

format (a4,3(1x,e9.2),3(1x,i9), (1x,e9.2))
ntest is a key word indicator, this card repeats for the current
injection quarter until ntest=endq
The next injection quarter is started and repeated, etc.
until ntest=endi, end of injections, then a computation
is done.
ntest is then read to determine if to end the run or to
return for a new set of injections

ntest=equt if this injection is equatorial
=polr if this injection is polar
=endq if completed this quarters injections

=endi *if completed all injections*

=next if to go back for new start quarter and year

=endr if run is to be terminated

(note: there must be at least one card with ntest=equt or polar followed by either ntest=endq or endi, then by ntest=endr)

ty=yield in Mtons for weapon

ff=fission fraction for weapon

hob=height of burst for weapon

twh=total number of weapons for this burst

nf =0 if only weapons on this burst

=1 if attack on reprocessing plant, *10-yr high level storage*

=2 if attack on 30-day spent fuel storage

=3 if attack on 3600 MW(th) LWR, (steady state)

=4 if attack on 10-yr spent fuel storage at reactor

nff=number of the above nuclear facilities under attack with this burst if nf = 0

detl=latitude of detonation, $0. \leq detl \leq 90$ (only northern latitudes may be used).

The computation will then proceed. The high-speed printer file will be named hi1111111 or if a file by this name exists, a new file name (incremented by 1) will be created. The graphics output will be in a standard F3yyyy0x file where yyyy is randomly chosen by the computer operating system.

The following example input deck is the same as the U.S.S.R. portion of the exchange used in Section 4.2.

Sample input deck of card images

```
5 0.70
n35.68   1560.00 n51.48     583.00 s33.87     1200.00 n45.47    970.00 n38.72    701.11
  0        200       0.33    1 1 1 1 2
 1.0e-7          1.00
    1.00      100.00            0.10     1000.00
  24    10    24
 225    10   225
1 1985
polr      0.90        0.50          0.00        916          0          0        39.00
polr      0.90        0.50          0.00         41          3        100        39.00
polr      0.90        0.50          0.00         42          4        100        39.00
polr      0.90        0.50          0.00          1          1          1        39.00
polr      0.90        0.50       1500.00       1000          0          0        39.00
polr     20.00        0.50          0.00         55          0          0        39.00
polr      0.75        0.50          0.00         30          0          0        39.00
polr      0.75        0.50       1000.00         30          0          0        39.00
polr     20.00        0.50       3000.00          3          0          0        39.00
polr      0.55        0.50       1000.00        000          0          0        39.00
polr      1.00        0.50       1500.00        100          0          0        39.00
polr      1.00        0.50          0.00         00          0          0        39.00
polr      0.20        0.50       1000.00         21          0          0        39.00
endi
endr
```

The current GLODEP2 controllee requires 443201 (octal) words. The drop-file requires 405400 (octal) words, about 14% of core on the Cray-1 computer. The run time of the code is dependent on the number of injections, the number of times a nuclear facility is attacked, and the number of specific locations at which to compute dose.

The sample calculation for Section 4.2 using an input deck with 9 additional injections to simulate the U.S. attack at 50 degrees latitude required 1.36 minutes of run-time.

0226G